NASA TECHNICAL MEMORANDUM NASA TM-75397

RESEARCH ON MEDIUM AND HIGH TEMPERATURE SOLAR HEAT STORAGE MATERIALS

Heine, D.,Jucker, J., Koch, D., Krahling, H., and Supper, W.

Translation of "Untersuchung von Mittel- und Hochtemperatur-latentwärmespeichermaterialen," Institut für Kerntechnik und Energiewandlung E.V. Stuttgart, W. Germany, Report No. IKE 5TF-258-78. (Research Contract No. 379-77-10 EED) (Periodic Report for period January 1, 1978 to June 30, 1978), July 1978, pp1-56

NATIONAL AERONAUTICS AND SPACE ADMINISTRATION
WASHINGTON, D.C. 20546 APRIL 1979

STANDARD TITLE PAGE

1. Report No. NASA TM-75397	2. Government Accession No.	3. Recipient's Catalog No.
4. Title and Subtitle Research on Medium and High Temperature Solar Heat Storage Materials.		5. Report Date April 1979 6. Performing Organization Code
7. Author(s) Heine,D., Jucker,J., Koch,D., Krahling,H., and Supper,W.		8. Performing Organization Report No. 10. Work Unit No.
9. Performing Organization Name and Address Leo Kanner Associates P.O.Box,5187, Redwood City,CA 94063		11. Contract or Grant No. NASW-3199 13. Type of Report and Period Covered Translation
12. Sponsoring Agency Name and Address National Aeronautics and Space Agency Washington,D.C. 20546		14. Sponsoring Agency Code

15. Supplementary Notes
Translation of "Untersuchung von Mittel- und Hochtemperatur-latentwärmespeichermaterialien" Institut für Kerntechnik und Energieumwandlung E.V. Stuttgart,West Germany,Report No. IKE 5TF-258-78.(Research Contract No. 373-77-10 EED) Periodic Report for period January 1,1978 to June 30,1978) July,1978, pp 1-56

16. Abstract

The three parts of the report deal with characteristics of solar heat storage materials,preliminary tests in which melting and solidification characteristics are tested and finally with service life and cycling tests.Various aspects of corrosion are discussed as well as decisions about ultimate selection of materials and a program for storage and evaluation of data.

17. Key Words (Selected by Author(s))	18. Distribution Statement Unclassified		
19. Security Classif. (of this report) Uncl.	20. Security Classif. (of this page) Uncl.	21. No. of Pages	22. Price

Project leader: Dipl. Ing. D. Heine

Associates: Dr. J. Jucker, Dr. D. Koch, Dipl. Ing. H. Krähling
W. Supper, M.S.

Technician: R. Kreutzburg

SUMMARY

This report deals with research of middle and high temperature solar heat storage materials. The report consists essentially of three parts.

Part one deals with the characteristics of solar heat storage materials. The general characteristics are discussed briefly. Characteristics to be investigated, like behavior during melting and during corrosion, are discussed in more detail. Particular attention is paid to the melting temperature, the melting period and to supercooling, as melting characteristics. Concerning corrosion the treatment of electrochemical reactions, of the rate of corrosion and of the types of corrosion are discussed in particular detail. Concerning thermal decomposition the discussion deals primarily with its possible causes.

Part two deals with preliminary tests during which melting and solidification characteristics are tested in simple heating and cooling tests. These investigations served as aid in making decisions about the ultimate selection of storage materials suitable for service life and cycling tests.

Service life and cycling tests are described at the end. A program for the storage of data and one for evaluation are discussed in particular detail in this part.

Table of Contents

1. Introduction

The general scarcity of available primary energy requires the exploitation of new energy sources as well as more economical handling of energy, resp. its optimum use. The sun represents an energy source with inexhaustible reserves that can be used without harm to the environment. The intelligent application of solar energy as well as a rational utilization of conventional energy generating equipment presupposes the employment of energy, resp. heat accumulators.

Various methods are possible for heat storage. One can essentially differentiate between the following groups:

1. Sensible storage: Materials with the highest possible specific heat c are raised to a higher temperature level while being charged and then cool off during discharge. Conventional storage media are water (c = 1.0 kcal/kg K) and siliceous embankments (c = 0.2-0.25 kcal/kg K).

2. Solar heat storage: Heat is stored here in the form of latent phase change heat. Phase transitions of solid-solid, solid-liquid, solid-gaseous and liquid-gaseous are possible. At present accumulators with a solid-liquid phase change are researched and constructed for the most part. During charging the storage medium is melted and during discharge it solidifies. Storage media are substances with high heat of fusion. In the temperature range to about 100°C that includes hydrated salts, paraffins, fatty acids and waxy esters, for higher temperatures it means inorganic salts without crystalline water, salt compounds, oxides, hydroxides, hydrides and metals.

3. Adsorption accumulators: During the charging process the adsorbed substance is evaporated, during discharge it condenses and is subsequently adsorbed. An example is silica-gel as absorption medium with water as the material to be adsorbed.

4. Chemical storage: During reversable chemical reactions the chemical heat of reaction is stored, resp. released after the reaction.

Metal hydrides can be mentioned here as examples where the reaction proceeds like

$$2\ Me + nH_2 \rightleftharpoons 2\ MeH_n \qquad (1)$$

Hydrogen is bound under release of heat (exothermic reaction) in the discharge cycle--and split off with the supply of heat (endothermic reaction)--in the charge cycle.

Each of these types of storage has its advantages and disadvantages. Solar heat accumulators excel by their high storage capacity per unit volume and mass volume, the small temperature difference between charge and discharge, the favorable temperature range for application and their low maintenance.

For construction of solar heat accumulators without problems it is necessary, however, to research a few more of the chemical and physical characteristics of storage materials. In the study to be made corrosive behavior with regard to construction materials, behavior during melting as well as the thermal stability of storage materials, will be investigated.

2. Characteristics of Materials for Solar Heat Storage

2.1 General characteristics

Among the characteristics that determine the selection of a storage material are:

1. Phase conversion enthalpy h_u (for solid-liquid change: heat of fusion is L):
   The larger h_u the larger the storage capacity.

2. Phase conversion temperature resp. melting temperature T_S:
   T_S should be as close as possible to the operating temperature.

3. Change of density during phase changes (volume change):
   Significant density changes during a change of phase can cause considerable pressure in the storage area with possible mechanical failure of the construction materials.

4. Specific heat:
   High specific heat in the liquid and solid states can add considerably to the storage capacity.

5. Density:
   The greater the density the smaller the storage volume and with it the storage installation.

6. Heat conductivity:
   Heat conductivity in the solid and liquid states influences the time for charge and discharge and determines the maximum distances for heat transfer surfaces.

7. Behavior during melting:
   The appearance of broad melting periods as well as of considerable supercooling of storage media must be avoided since too great differences will otherwise occur during charge and discharge.

8. Thermal stability:
   The solar heat accumulators should work maintenance-free for at least 20 years. The expectation is that the storage medium is insensitive to repeated phase changes and occasional major overshooting of the melting point.

9. Compatibility with construction materials:
   In the design of solar heat accumulators it is important that the storage medium not attack the construction material.

Sufficient results, resp. data from previous investigations are available for the majority of characteristics listed. But very little is known about the behavior during melting and corrosion, or about the thermal stability, of storage media.

2.2 Behavior during melting and solidification

2.2.1 Melting temperature and melting period

Melting and solidification characteristics of the storage media, given the assumption that melting and solidification behavior agree, are of decisive influence on the operation of the accumulator. The operational temperature of the storage system should agree with the melting temperature of the storage medium. The melting temperature can only be influenced through the choice of storage media since the melting temperature of elements and compounds is practically independent of pressure.

Multiple mixtures consisting of several elements and/or compounds have no constant melting temperature, i.e., no melting point but rather a melting period, eutectic compounds being the exception. The melting period is limited by the temperatures of the liquid state above which the entire mixture is melted, and of the solid state temperature below which the whole mixture solidifies. Between these two temperatures a mixture of solid and liquid phases exists. The temperatures of the liquid and solid state depend on the composition of the mixtures and on pressure; the length of the melting period depends only on the composition. Long melting periods are unsuitable for solar heat storage since they make the temperature difference between charge and discharge of the accumulator too great.

Additional disturbing characteristics are: the tendency of some materials to supercooling during solidification and the occasional decomposition of mixtures after repeated cycles of melting and resolidification.

2.2.2 Supercooling

The driving force of each phase change is the difference of free enthalpy between the initial and the final phase. As soon as a change has set in the atoms of the final phase will assume positions corresponding to the lower enthalpy by way of diffusion or by cooperative atom motions. The new and old phases are separated by a boundary area, which is formed by the generation of boundary area energy.

If we look at a spherical particle of the solid phase in the melt with radius r, then the gain of free enthalpy is

$$-\frac{4}{3}\pi r^3 G_V \qquad (2)$$

G_v is the difference in specific free enthalpy (with reference to the volume) between the solid and liquid phases. Energy in the amount of

$$4\pi\ r^2\ \gamma \tag{3}$$

must be generated to form the boundary area. γ is the specific boundary area energy (referred to the surface).

The entire change ΔG of the free enthalpy is thus:

$$\Delta G = -\frac{4}{3}\pi\ r^3\ \Delta G_v + 4\pi\ r^2\ \gamma \tag{4}$$

Fig. 1 shows this function. It reaches a maximum for the critical radius r_k. That means particles larger than r_k continue to grow without energy supply from the outside and are therefore designated as nuclei; r_k is the critical nucleus size. Energy must be expended until r_k is reached, since the boundary area term predominates when r is small.

The work required for generation of a nucleus with radius r is called the nucleus formation work A. A and r_k can be calculated from equation (4).

$$A = \frac{\Lambda 6\pi\ \gamma^3}{3(\Delta G_v)^2} \tag{5}$$

$$r_k = \frac{2\gamma}{\Delta G_v} \tag{6}$$

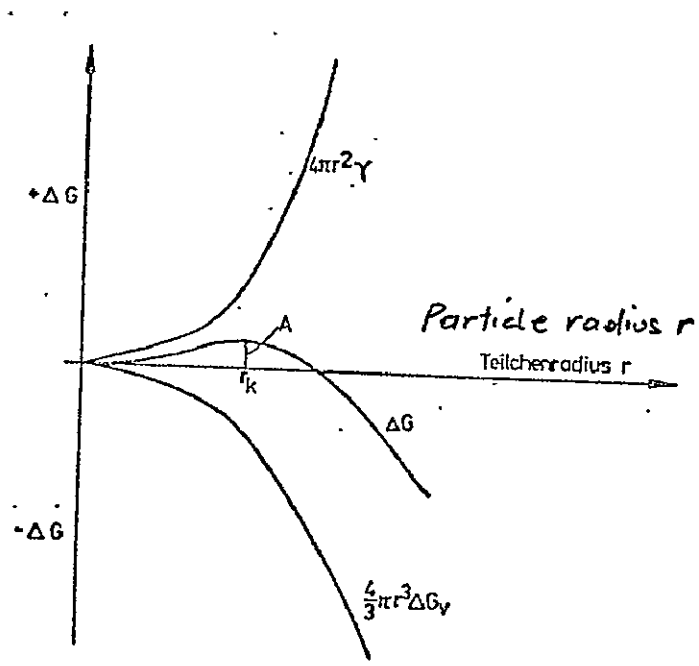

Change of free enthalpy as function of the particle radius during a phase change

Änderung der freien Enthalpie in Abhängigkeit vom Teilchenradius bei einer Phasenumwandlung.

Fig. 1. Phase change.

The dependence of the critical nuclear radius r_k and of the nucleus generating work A on the temperature is important. Since the energy of the boundary area may be considered as largely independent of temperature, ΔG becomes the parameter that determines temperature dependence. ΔG is written as

$$\Delta G_V = \Delta H - T\Delta S,$$

where H is enthalpy and S is entropy. For the phase change temperature (melting temperature) T_S $\Delta G = 0$ and therefore

$$\Delta H = T_S \Delta S$$

where ΔH is the heat of transformation (melting heat). From this follows

$$\Delta G_v = \frac{\Delta H\ (T_S - T)}{T_S}$$

The critical nuclear radius r_k and the work for nucleus generation, A, can then be written as

$$r_k = \frac{2\gamma\ T_S}{\Delta H(T_S - T)} \tag{7}$$

and

$$A = \frac{\Lambda 6\pi\ \gamma^3\ T_S^2}{3(\Delta H)^2(T_S - T)^2} \tag{8}$$

$T_S - T$ is simply supercooling.

It has been shown that all particles smaller than r_k are thermodynamically unstable. The question arises as to how particles of critical size, i.e., nuclei, are generated.

As our point of departure we assume that in the initial phase (melt) a number of atoms is always arranged so that the arrangement will largely correspond to the new (solid) phase. The size of these "subcritical particles," often called embryos, is temperature dependent. The size of the available particles increases with increasing supercooling. Nucleus generation starts when supercooling becomes so great that the "subcritical particles" have reached size r_k. This corresponds to the point of intersection x in Fig. 2. The procedure so far described corresponds to homogeneous nucleus generation where initially no location favoring nucleus generation exists. Most nucleus generation occurs as heterogeneous procedures with nucleus formation in the new phase on available boundary surfaces.

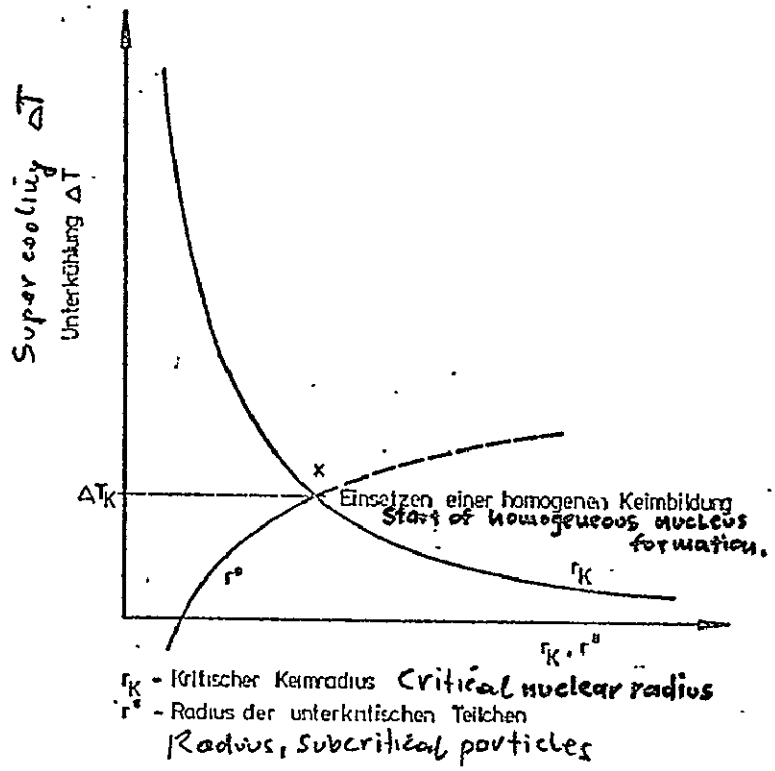

Fig. 2. Homogeneous nucleus generation, influence of supercooling.

During solidification the nucleus formation can take place at the container wall, on solid foreign particles, or on deliberately added seed crystals. The amount of promotion of nucleus formation by the available boundary surfaces depends on the structure of the latter. The greater the agreement of the lattice structure and lattice spaces between available boundary surfaces and the phase to be formed, the more effective will the foreign nuclei be during the liquid-solid transformation.

Energy needed from outside for the formation of the boundary surface is reduced for heterogeneous nucleus formation and so is the work required for nucleus formation as well. In consequence supercooling required for employment of nucleus formation is much smaller than for homogeneous nucleus formation. This means that it can be suppressed by judicious addition of foreign nuclei at the onset of supercooling.

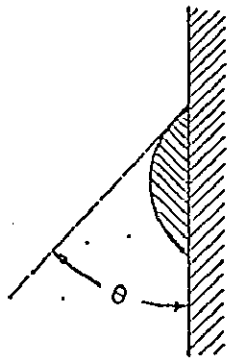

Nucleus formation at a wall

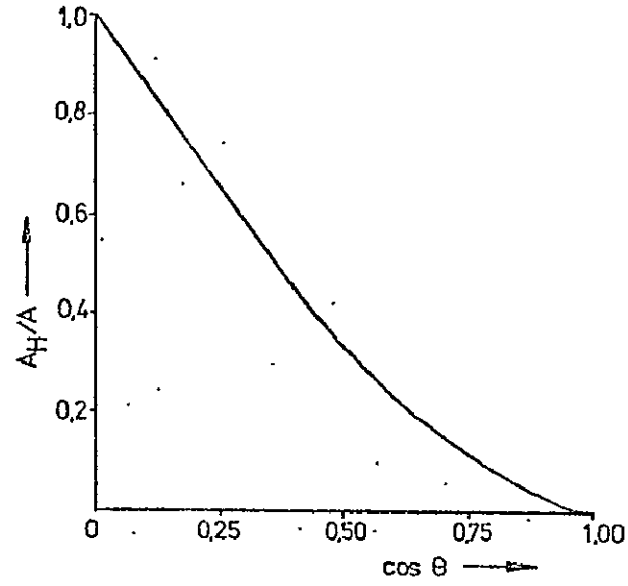

Ratio of work for heterogeneous nucleus formation A_H, to work for homogeneous nucleus formation A, as a function of the boundary angle θ of wetting

Fig. 3. Heterogeneous nucleus generation.

2.3 Thermal decomposition

By the concept of thermal decomposition we understand all phenomena of decomposition and disassociation of storage materials that are caused by thermal stresses and the melting process. A few reasons for decomposition can also be considered as melting characteristics, but they are dealt with as thermal decomposition because of their effects. Only materials that do not experience thermal decomposition, i.e., those that are thermally stable, are suitable for storage materials.

To start with several examples of decomposition caused by thermal stress will be listed.

It is known that carbonates decompose at high temperatures. The reaction occurs according to

$$Me_n(CO_3)_m \longrightarrow Me_nO_m + mCO_2 \qquad (9)$$

Nitrate and nitrite are not stable at temperatures above 500°C. They also decompose above that temperature. The following reactions may occur:

$$\begin{aligned} 2\ Me\ NO_3 &\longrightarrow 2\ Me\ NO_2 + O_2 \\ 2\ Me\ NO_2 &\longrightarrow Me_2O + NO + NO_2 \end{aligned} \qquad (10)$$

These reactions apply for pure salts and salt mixtures. During the melting of salt mixtures additional decomposition, resp. dissociation, can take place based on their phase relations, phase transformations, different physical characteristics and their density.

When a solid solution or compound made up of components of varying density is melted down, separations occur in the fluid

state. The components are layered according to their density. This phenomenon is known as segregation by weight.

The thermodynamic conditions during melting and solidification of multiple material systems are stated in the phase diagram. In the main the following systems are recognized:

a. with complete solubility in the solid and liquid states

b. with complete solubility in the liquid state, insolubility in the solid state

c. with complete solubility in the liquid state, and limited solubility in the solid state

d. with limited solubility in the liquid state

e. with generation of compounds.

Fig. 4 shows all systems of interest for solar heat storage materials. These are binary systems; for multiple systems conditions are similar. Mixtures with complete solubility in the liquid and solid states (Fig. 4a) are of interest for solar heat storage when a melting period can be taken into consideration. Systems with minimum melting points form the exception (Fig. 4b). Dissociations are out of the question for such systems. At the minimum melting temperature small shifts of concentration may occur so that the possibility of short melting periods exists.

In systems with unlimited and limited solubility mixtures of eutectic compositions are interesting (Fig. 4c and d). They have a fixed temperature for melting and solidification and are thermally stable with regard to melting. If only α-crystals, resp. A-crystals, separate out in the melt then the melt will

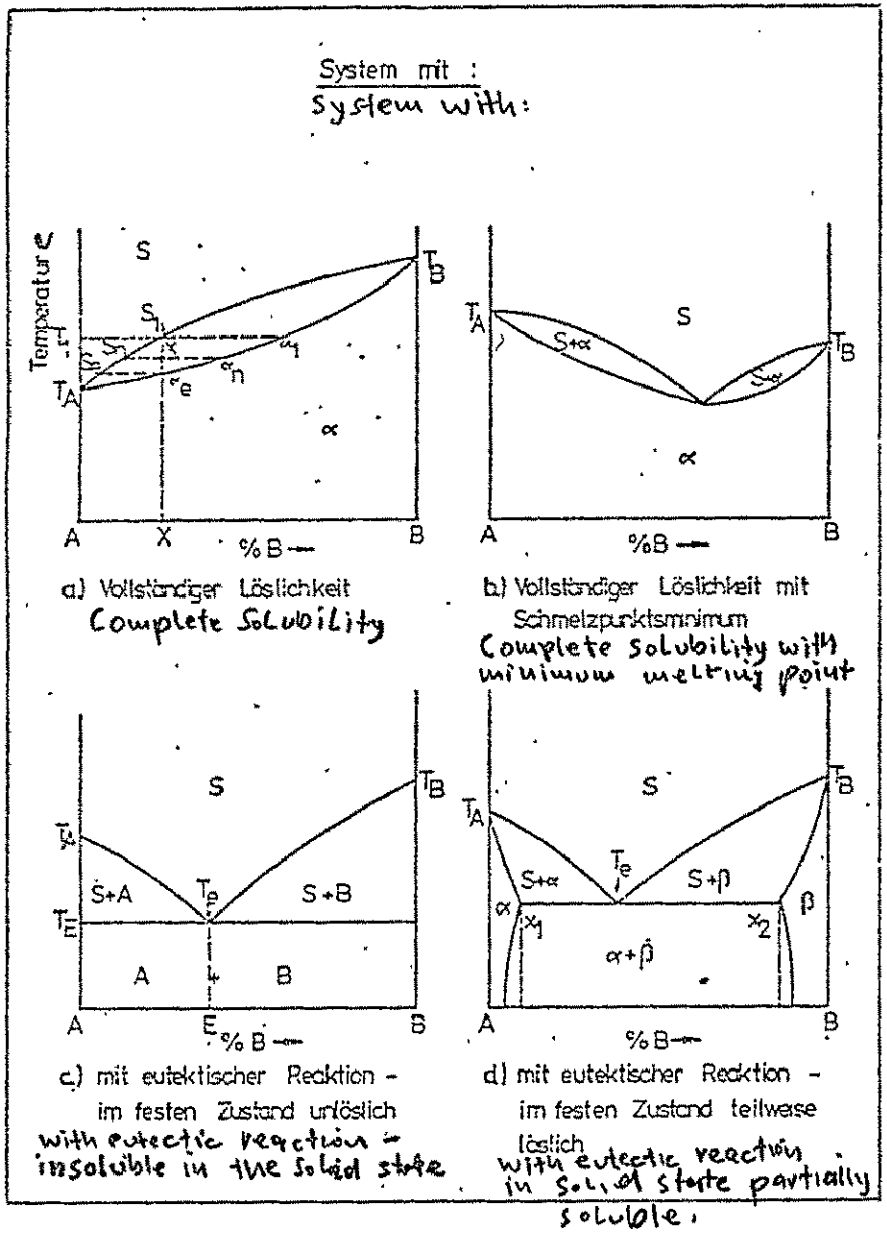

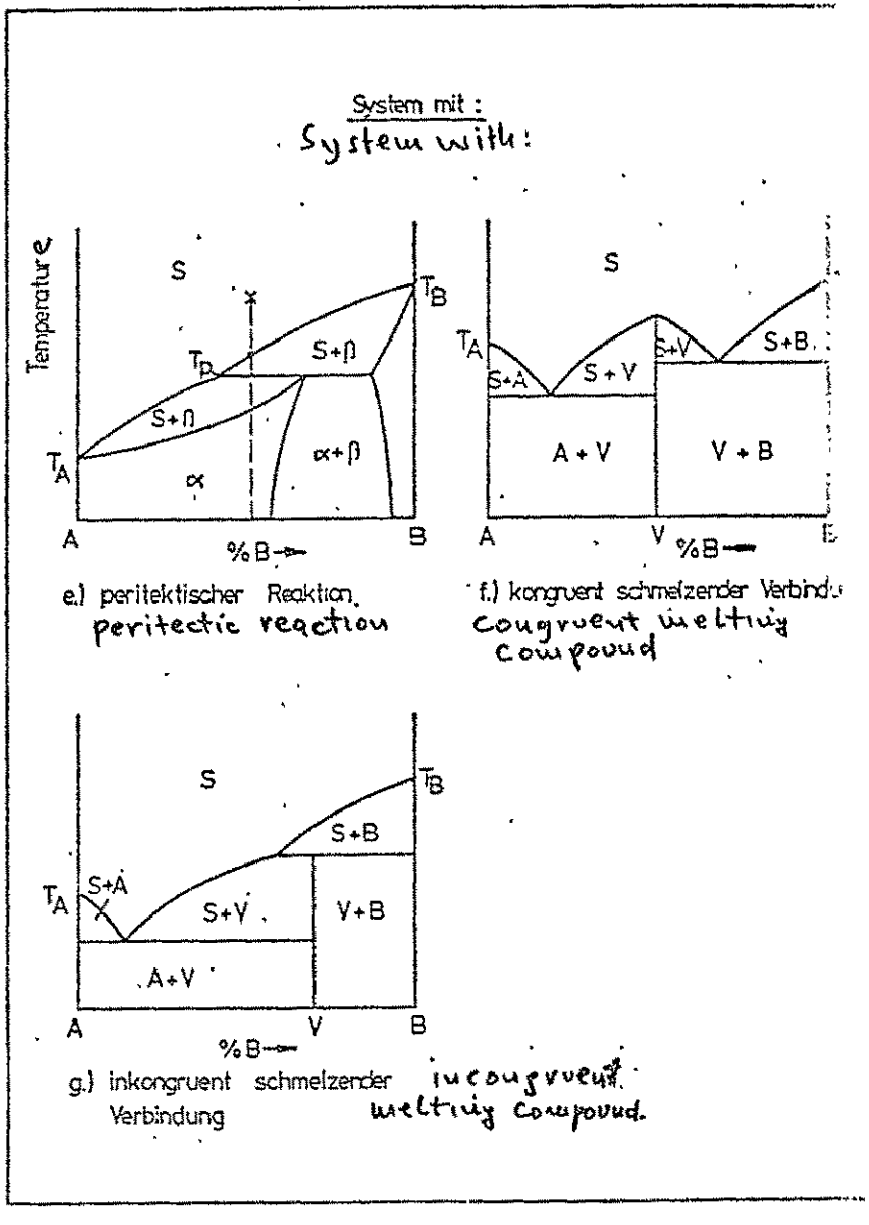

Fig. 4. Phase diagram.

Bild 4: Phasendiagramme

experience a paucity of A-atoms, i.e., the condition changes in favor of the B-atoms. But this causes an increase in the probability of nucleus formation for the β-, resp. B-phase so that even when only α and A nuclei are formed at first it must be expected that nucleus formations of the β-, resp. B-phases, will follow immediately.

If peritectics (Fig. 4e) appear in the solid state of systems with limited solubility, dissociations can occur in such compounds. It is characteristic for a peritectic reaction that β-crystals, first discarded by the melt, will react with the melt to a second phase α.

$$S + \beta \longrightarrow \alpha \qquad (11)$$

Looking at a salt of concentration X, which consists only of the α-phase in the state of equilibrium after solidification, peritectic reaction T_p starts when the peritectic temperature T_p gets to the boundary surface β/melt. The β crystals are surrounded by an α-seam.

If the reaction is to progress then B-atoms of the β-phase must diffuse through the α-layer to the melt, or A-atoms of the melt must diffuse through the α-layer to the β-phase. The rate of reaction is determined by the speed of diffusion in the solid α-phase. Complete peritectic reaction during solidification will only occur for very slow cooling rates. In the other case β-crystals surrounded by α-crystals are present in the solid state. Since slow cooling is not guaranteed when the appropriate salts are applied in the operation of the solar heat accumulator, suppression of the peritectic reaction may occur and with it the presence of two solid state phases. That can change the melting behavior of the storage medium considerably when repeated melting and solidification takes place.

Among systems with formation of compounds we differentiate between those that have congruently melting compounds and those where the compounds melt incongruently (Fig. 4f and g). Compounds that melt congruently are suitable as storage media since no dissociation is expected of them. An incongruently melting compound V decomposes in a peritectic reaction into a phase B and a liquid phase S, melting completely as soon as it reaches the liquidus temperature. During solidification the same processes occur that were described previously. Here, too, dissociation can happen, leading to changes in the melting behavior.

The decomposition and dissociation processes described can all occur together. It is entirely possible that during long-term operation dissociations in combination with density differences of the components will lead to segregations.

2.4 Corrosion

2.4.1 Electrochemical reaction and rate of decomposition

Corrosion of metallic materials by melted salts corresponds to corrosion of metallic materials in highly concentrated aqueous solutions. The corrosion of metals in aqueous solutions is an electrochemical reaction consisting of two partial reactions. The anodic reaction (oxidation)

$$Me \longrightarrow Me^{n+} + ne \qquad (12)$$

which dissolves the metal and the cathodic reaction (reduction)

$$nH^{+} + ne \longrightarrow \frac{n}{2} H_2 . \qquad (13)$$

Both processes can take place on various locations on the metal surface but they are always coupled with each other in

electrochemical balance. These separate corrosion processes are best shown in a graphic illustration of current density vs. potential. Fig. 5 shows the experimentally measured total current density curve i_g by addition of the anodic (i_a) and cathodic (i_k) current density curves. Current i_g goes through 0 at a corrosion potential of E_{ko}. This point represents a state of equilibrium. Corrosion current density i_{ko} is defined by

$$i_{ko} = i_a = |i_k|$$

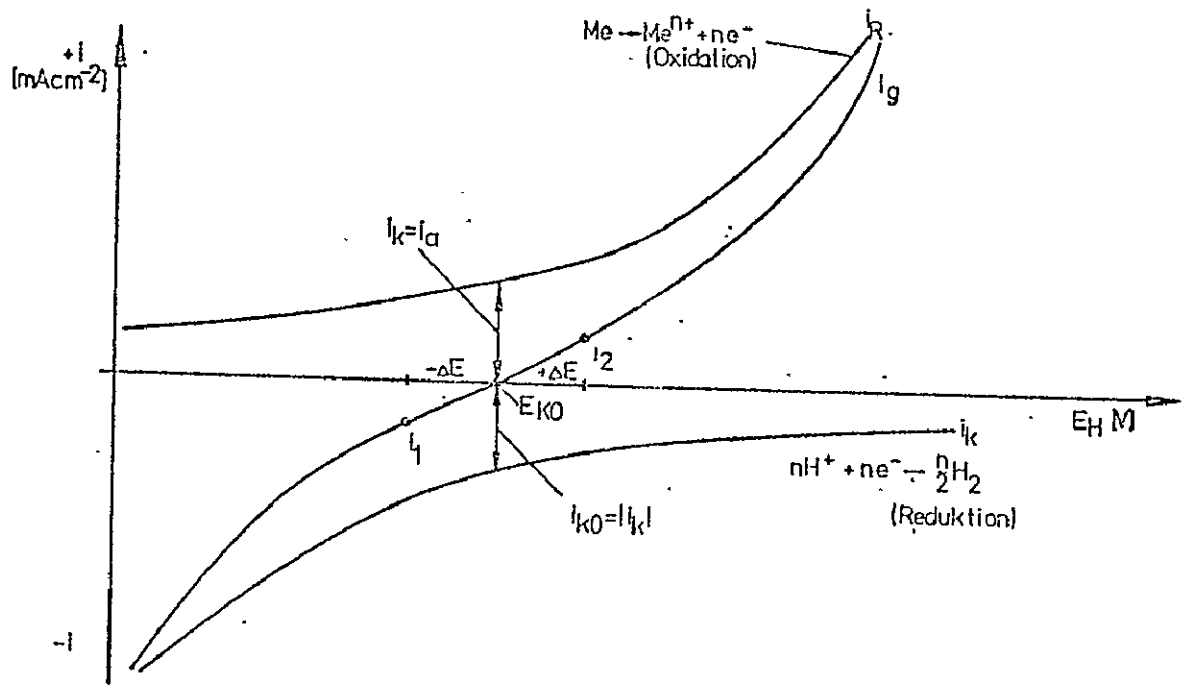

Fig. 5. Current density-potential, graphic illustration.

Corrosion current density i_{ko} is also defined as decomposition rate and it determines the extent of corrosion. It is important to know the contribution of the corrosion current for evaluation of the corrosion processes. Two methods will be

explained briefly. According to Engell /12/, a potential $\pm\Delta E$ (10 mV) is superimposed on the corrosion potential E_k and, using the current density-potential diagram with a potentiostat and a ΔE voltage regulator, points i_1 and i_2 on the i_g curve are obtained. The desired current density i_k is then calculated as

$$i_{ko} = \frac{i_1}{\cdot \exp(\beta \Delta E - 1)} = \frac{i_2}{1 - \exp(-\beta \Delta E)} \qquad (14)$$

with $\beta = \frac{\alpha \; z \; F}{R \; T}$

Z = valence of ions
F = Faraday constant
α = leakage factor (0.5)

The rate of decomposition can also be determined by means of the weight loss caused by the corrosion. Advantage is taken here of the proportionality between current and the dissolved amount of metal Δm. According to Faraday's 1. Law:

$$\Delta m = \frac{\ddot{A}}{F} \; I \quad t \qquad (15)$$

Ä is the weight equivalent, I is the current and t the time

$$i_k = \frac{F \cdot \Delta m}{\ddot{A} \cdot t \cdot A} \qquad (16)$$

A is the probe surface.

2.4.2 Types of corrosion

Types of corrosion, which can occur between storage materials and construction materials, will now be discussed.

2.4.2.1 Uniform surface corrosion

By uniform surface corrosion we understand nearly uniform reduction along the total surface. There must be no spots with increased corrosion.

The characteristic data for uniform surface corrosion are obtained through the mass loss. The parameters listed in Table 1 are required for that.

Table 1

Test Data Required for Determination of Surface Corrosion

Meaning	Symbol	Unit
Corroded surface	A	cm
Mass loss	Δm	g
Density	P	$g.\ cm^{-3}$
Period of load	t	h or d

Corrosion parameters listed in Table 2 can be calculated from the test data.

Table 2

Meaning	Symbol	Unit
Rate of mass loss referred to the surface	Δm_A	$g.m^{-2}$
Thickness decrease	ΔS	μ m
Rate of mass loss referred to the area	V	$g.m^{-2}.h^{-1}$ $g.m^{-2}.d^{-1}$
Rate of removal	W	$mm.a^{-1}$ 1)
1) 1a = 365d		

The value of mass loss referred to the area

$$V = \frac{\Delta m}{A \cdot t} \qquad (17)$$

is proportional to the rate of decomposition (equation (16)). If the mass loss rate, as referred to the area, reaches constant values as function of time estimates for the service life of technical components are possible. Area-related mass loss rates of materials with different densities cannot be compared with one another. For such comparisons the decrease in thickness for equal periods of service, or the rate of removal, w, is more suitable.

$$w = \frac{V}{\varrho} \qquad (18)$$

According to the Dechema-Material Tables the following guidelines are valid for the evaluation of materials:

Corrosion resistant	Removal rate	$\leq$0.1 mm/a
Fairly resistant	Removal rate	$\leq$1.0 mm/a
Not very resistant	Removal rate	$\leq$2.5-3.0 mm/a
Unsuitable	Removal rate	$\leq$3.0 mm/a

2.4.2.2 Hole and trough corrosion

Localized corrosion leading to corrosion troughs, resp. holes, is designated as hole and trough corrosion in the broadest sense.

Localized attack by which metals in a passive state can be affected, is considered as hole corrosion in its particular meaning. Ions of the halogenides Cl^-, Br^- and J^- are capable of destroying passive layers locally. This is a dangerous corrosion attack since mass losses of any consequence are rarely observed

when it occurs and since often no noticeable changes are apparent at the metal surfaces while small,but very deep, holes are eaten into the material. Starting point for hole corrosion may be macroscopic faults and microscopic disturbances (displacements, grain boundaries).

Hole corrosion by halogens is particularly frequent in highly alloyed Cr and NiCr-steels, in aluminum alloys, as well as in titanium, nickel and their alloys.

2.4.2.3 Intercrystalline corrosion

Intercrystalline corrosion is a selective attack that takes place preferentially at grain boundaries, resp. areas close to grain boundaries. The attack proceeds from the surface downwards, leading in its final stage to total decomposition of the material into individual crystallites. The cause of intercrystalline corrosion must be sought in the susceptibility of grain boundaries to corrosion.

Austenitic steels are sensitive to intercrystalline corrosion. During heating of homogeneous austenitic steels to temperatures between 450°C-850°C, when welding for instance, chromium carbide will separate out along the grain boundaries. This impoverishes the crystal structure in those areas of dissolved chromium below the critical level. Corrosion elements are formed under the influence of certain electrolytes, between the chromium-rich grain centers and those areas. The intercrystalline attack can be prevented by very low carbon contents or by stabilization of the steels with the elements Ti, Nb or Ta.

2.4.2.4 Stress corrosion

An equally dangerous type of corrosion is the stress corrosion. This one also occurs often without visible change in the metal surface. Like the hole corrosion it appears predominantly in metals that form a cover layer, for instance low and high alloyed steels, nickel alloys, aluminum, brass or magnesium. The prerequisite for this type of corrosion is the interaction of three items:

1. a material sensitive to stress tension

2. the action of a specific electrolyte

3. the presence of static external or internal stresses.

The corrosion medium destroys the cover layer at weak spots (glide steps, permutations, grain boundaries, microfissures, etc.) and surface notches are generated. Where such a notch is at right angles to a tensile strain, a stress σ_k exists in it which is greatest at the bottom. When the stress exceeds the yield point fissures will develop if there are enough sharp notches. These fissures will spread throughout the interior of the material. The direction of the fissures can be transcrystalline (for very high stresses) as well as intercrystalline (the conditions are the same as for intercrystalline corrosion without stresses).

3. Preselection

3.1 Storage materials

In the preselection of storage materials the characteristics discussed in section 2 were considered as much as possible. The

heat of fusion and the melting temperature did form the focal points, however. Care was taken to select particularly such storage materials which have a melting point and no melting period, i.e., predominantly simple salts and eutectic mixtures.

For the final selection costs and availability of suitable substances should be considered, based on available information. In Tables 3 and 4 a few of the inorganic compounds, suitable as storage materials for the medium and high temperature range, are listed separately. Only those characteristics were included in the tables for which data were available for all compounds. Table 5 contains a few mixtures that seem suitable as storage materials. Assembly of the data showed that for a few important characteristics values were not available for all the listed compounds and mixtures.

Table 3

Materials for Medium Temperature Latent Heat Storage, 200-245°C

Name	Formula Formel	Melting Point resp. Range Schmelzpunkt bzw Bereich °C	Molecular Weight Molekular-Gewicht	Density Dichte $g cm^{-3}$	Heat of Fusion Schmelzwärme kJg^{-1}	Crystal Structure Kristallstruktur
Aluminiumchloride	$AlCl_3$	192	133,34	2,44	0,2587	monoklin C
Lithiumnitrate	$LiNO_3$	250[1], 264[3]	122,98	2,36	0,3699	trigonal R
Natriumnitrate	$NaNO_3$	310,5[1], 307[3]	84,99	2,26	0,1718 [1] 0,2636 [2]	trigonal R
Zinkchloride	$ZnCl_2$	318[1], 283[3] 313[2]	136,28	2,91	0,1688 [1] 0,3797 [2]	tetragonal I
Natriumhydroxide	NaOH	319,1	40,00	2,15	0,1590	orthorhomboedr. C
Lithiumhydroxide	LiOH	445 [1], 450 [3] 471 [2]	23,95	1,43	0,8768	tetragonal P
Boroxide	B_2O_3	460-470	69,62	1,84	0,3304	kubisch cubic

Literature: [1] D'Ans, Lax: Chemiker-Taschenbuch 3Aufl Bd 1; [2] Gmelin Handbuch der anorganischen Chemie
[3] West, R.C: Handbook of Chemistry and Physics

Table 4

Materials for High Temperature Latent Heat Storage, 600-950°C

Name	Formula Formel	Melting Point resp. Raure Schmelzpunkt bzw Bereich °C	Molecular Weight Molekular-Gewicht	Density Dichte gcm^{-3}	Heat of Fusion Schmelzwarme kJg^{-1}	Crystal Structure Kristallstruktur
Iron Eisen(II)-Chloride	$FeCl_2$	677 [1]	126,75	2,98	0,3393	trigonal R
Lithiumhydride	LiH	686 [1,2] 680 [3]	7,95	0,77	3,6855	cubic kubisch F
Lithiumcarbide	Li_2C_2	699 [1,2]	37,90	1,65		
Magnesiumchloride	$MgCl_2$	714 [1,2], 708 [3]	99,22	2,41	0,4526	trigonal R
Calziumchloride	$CaCl_2$	782 [1,2], 772 [3]	110,99	2,15	0,2645	orthorhomboedr. P
Sodium Natriumchloride	NaCl	800 [1,2]	58,54	2,16	0,4928	cubic kubisch F
Lithiummetaborate	$LiBO_2$	836 [1], 845 [3]	49,75	2,22	0,6231	triklin
Lithiumflouride	LiF	848 [1], 842 [3]	25,94	2,64	1,0177	cubic kubisch F
Sodium Natriumcarbonate	Na_2CO_3	854 [1], 852 [3]	105,99	2,53	0,3113	
Potassium Kaliumfluoride	KF	857 [2], 846 [3]	58,10	2,37	0,4521	orthorhomboedr. C.
Sodium Natriumsulfate	Na_2SO_4	884 [1]	142,04	2,70	0,2021	orthorhomboedr. F

Literature: [1] D'Ans, Lax: Chemiker-Taschenbuch 3 Aufl Bd 1 ; [2] Gmelin, Handbuch d anorganischen Chemie
[3] West, R C: Handbook of Chemistry and Physics

Table 5

Mixtures of Inorganic Compounds for a Latent Heat Storage

Mixture Mischung	Melting Point resp. Period Schmelzpunkt bzw-intervall °C	Heat of Fusion Schmelzwarme kJkg^{-1}	Density Dichte gcm^{-3}
KOH-NaOH	190	233	2,06
NaCl-ZnCl	260	198	248
NaCl-Na_2CO_3-NaOH	282	316	2,10
KCl-$MgCl_2$-NaCl	396	412*	2,25*
$MgCl_2$-NaCl	435	328	2,16
KF-NaF	710	479	2,51
KF-MgF-NaF	809	603	2,63

Values from:
Werte aus: Tye, R.P., Bourne, J.G., Desjarlais, A O, Clark, P.V, Dean, C.D.
*berechnet calculated

It is remarkable that lithium compounds show very high fusion both temperature ranges. Their disadvantage is their high price/kg. $MgCl_2$, NaCl and KF, as well as the mixtures NaF-MgF_2-KF and KF-NaF, offer great fusion heat values for the temperature range 600-950°C.

There is no great difference in the fusion heat among the compounds and mixtures that do not contain lithium, for the medium temperature range. Only NaOH and the mixture NaCl-$ZnCl_2$ have low values. The melting points of the listed salts and mixtures are so positioned that both ranges are well covered.

3.2 Construction materials

The following points were of importance in the choice of construction materials:

a. Corrosion resistance with regard to possible storage materials, according to available data.

b. Applicability for appropriate operating temperatures (melting temperature of the storage medium).

c. Satisfactory strength characteristics to withstand eventual mechanical stresses due to volume changes of the storage medium during phase changes.

d. Availability, i.e., no specialized materials where possible.

Often no corrosion data for the melted salts were available, only for their aqueous solution. A satisfactory reply to the question whether the suggested materials are suitable as container

materials in combination with storage media can only be given after investigations have been carried out.

Tables 6 and 7 show materials for the temperature range 200-450°C. Table 7 contains the numbers of the materials, their DIN-nomenclature and chemical composition. Table 7 shows the physical and mechanical characteristics.

Table 6

Construction Materials for the Temperature Range 200-450°C, Chemical Characteristics

		Material Werkstoff	DIN-Designation DIN-Bezeichnung	German Material Number Deutsche Werkstoffnummer	Chemical Composition in % Chemische Zusammensetzung in %												
					C	Si	Cu	Zn	Fe	Mn	Cr	Sn	Al	Mo	Ni	S	P
Iron Materials	Eisen - Werkstoffe	St 35	St 35	1.0308	0,18				99,72							0,05	0,05
		St 37	St 37	1 0110	0,2				99,7							0,05	0,05
		13 CrMo 44	13 CrMo 44	1,7335	0,14	0,25			97,7	0,55	0,90			0,45		0,04	0,04
Copper Alloys	Kupfer - Legierungen	Cunifer 30	CuNi 30Fe	2.0882	0,05		65	0,5	0,6	1,0					31	0,02	
		SnBz 8	SnBz 8	-			92					8					
		Ms 80	Ms 80	2.0250			80	20									
Nickel Alloy	Nickel - Legierung	Monel	NiCu 30Fe	2.4360	0,15	0,5	31		1,8	1,25			0,5		63	0,02	

Table 7

Construction Materials for the Temperature Range 200-450°C

a) physical characteristics

		Material Werkstoff	Melting Range Schmelzbereich °C	Density Dichte gcm^{-3}	Heat Conductivity Wärmeleitfähigkeit Wm^{-1}K^{-1} bei 20°C at	Specific Heat Spezifische Wärme Jkg^{-1}K^{-1} bei 20°C at	Average Linear Expansion Coefficient Mittlerer linearer Ausdehnungskoeffizient 20 - 800°C x10^{-6}
Iron Materials	Eisen - werkstoffe	St 35	1450 -1520	7,85	48,14	470	12
		St 37	1450 - 1520	7,85	48,14	470	12
		13 CrMo44	1470 - 1505	7,85	41,80	470	13
Copper Alloys	Kupfer - legierungen	CuNi30Fe		8,90	30,00	376,7	16
		SnBz 8	880-1040	8,73	46,0		17,8
		Ms 80	900 - 950	8,25	117,2		18,5
Nickel Alloy	Nickel - legierung	NiCu30Fe	1320 -1375	8,85	25,95	527,7	17

b) mechanical characteristics

		Material Werkstoff	Streckgrenze bzw 02-Dehngrenze Nmm^{-2}		Zugfestigkeit Nmm^{-2}		Time Stretch limit Zeitdehngrenze $\sigma_{1/1000}$ Nmm^{-2}
			at Room Temp. bei Raumtemp.	at Higher Temp. b. höherer Temp.	at Room Temp. bei Raumtemp.	at Higher Temp. b. höherer Temp.	
Iron Materials	Eisen-werkstoffe	St 35	240		350-450		
		St 37	240		370-450		
		13CrMo44	300	at bei 500°C: 170	440-500	at bei 500°C: 170	
Copper Alloys	Kupfer-legierungen	CuNi30Fe	120-220	at bei 425°C: 98	370	at bei 400°C: 275	
		SnBz 8	-		400-700		
		Ms 80	-		270		
Nickel Alloy	Nickel-legierung	NiCu 30Fe	190	bei 425°C: 140 at	450-600		bei 420°C: 140 at

Copper and nickel alloys are suitable for the medium temperature range, in addition to unalloyed and low alloy steels; the latter because of their favorable price, the copper and nickel alloys because of their better conversion characteristics.

Materials for the temperature range 600-950°C are shown in Table 8 (chemical composition) and Table 9 (physical and mechanical characteristics). These are mainly heat resistant steels and resistance alloys. Cobalt alloys do not yet enjoy much distribution and are hard to procure.

Table 8

Construction Materials for the Temperature Rnage 600-950°C
Chemical Characteristics

		Material Werkstoff	DIN-Designation DIN-Bezeichnung	German Material Number Deutsche Werkstoffnummer	Chemical Composition in % Chemische Zusammensetzung in %											
					C	Si	Cu	Fe	Mn	Cr	Ti	Al	Co	Ni	S	P
Heat resistant Steels	hitzebeständige Stähle	Cronifer 2012	X15CrNiSi2012	1.4828	0,15	2,0		65,4	22	20	0,5					
		Nicrofer 3220 H	X10CrNiAlTi 3220	1.4876	0,07	<1,0	0,7	29	<1,0	21	0,4	0,4		32	0,03	0,03
Nickel Alloys	Nickel-legierungen	Nimonic 75	NiCr 20 Ti	2.4630	0,12	1,0	0,5	5,0	1,0	20				72,9		
		Nicrofer 7216	NiCr15Fe	24816	0,08	<0,5	<0,5	8	1,0	16	<0,3		<1,0	72	0,01	0,03

Table 9

Construction Material for the Temperature Range 600-950°C

a) physical characteristics

		Material Werkstoff	Melting Range Schmelzbereich °C	Density Dichte gcm^{-3}	Heat Conductivity Wärmeleitfähigkeit $Wm^{-1}k^{-1}$ bei 20°C at	Specific Heat Spezifische Wärme $Jkg^{-1}k^{-1}$ bei 20°C at	Average Linear Expansion Coefficient Mittlerer linearer Ausdehnungskoeffizient 20 - 800°C $\times 10^{-6}$
Heat resistant Steels	hitzebeständige Stähle	X15CrNiSi2012		7,80	14,65		18,5
		X10CrNiAlTi3220	1370 - 1400	8,00	11,70	500	18,0
Nickel Alloys	Nickel-legierungen	NiCr20Ti	1340 - 1380	8,37	11,70	461	16,5
		NiCr15Fe	1375 - 1520	8,50	15,10	460	15,9

b) mechanical characteristics

		Material Werkstoff	Stretch Limit Streckgrenze bzw 0,2-Dehngrenze Nmm^{-2}		Tensile Stress Zugfestigkeit Nmm^{-2}		Time Stretch Limit Zeitdehngrenze $\sigma_{1/1000}$ bei 600°C at Nmm^{-2}
			at Room Temp. bei Raumtemp.	at Higher Temp. b höherer Temp.	at Room Temp. bei Raumtemp.	at Higher Temp. b höherer Temp.	
Heat resistant Steels	hitzebeständige Stähle	X15CrNiSi2012	300		600 - 700		20
		X10CrNiAlTi3220	205	bei 550°C: 150 at	490		20
Nickel Alloys	Nickel-legierungen	NiCr20Ti	275	bei 800°C: 130 at	750	bei 800°C: 240 at	26
		NiCr15Fe	180	bei 425°C: 145 at	500		12

4. Experimental Investigations

4.1 Preliminary investigations

4.1.1 Design and performance of experiment

The purpose of this test series is the final selection of a few compounds and mixtures with thermal characteristics suitable for latent heat storage; these are later submitted to service life and cycle tests to obtain their long-term corrosion behavior in connection with metallic structural materials, resp. their melting characteristics as a consequence of decomposition during full-time operation.

Of immediate interest is the melting and solidification behavior of the selected salts. In addition to finding the melting point the appearance of melting, resp. solidification intervals, as well as possible supercooling of the melt during solidification, are investigated.

The following inorganic compounds and mixtures were investigated: $NaNO_3$, $ZnCl_2$, NaOH, B_2O_3, NaOH-KoH, KCl-$ZnCl_2$, KCl-$MgCl_2$-NaCl and NaCl-$MgCl_2$ in the medium temperature range and $MgCl_2$, NaCl, KF and Na_2SO_4 in the high temperature region.

The lithium compounds were not tested because of their high cost. Aluminum chloride and iron chloride were discarded because of their hygroscopic behavior. Calcium-chloride has a lower heat of fusion than potassium chloride with a melting point only 12°K above it, so it was not considered.

The investigation of NaCl-$NaCo_3$-NaOH, KF-NaF and MgF_2-KF-NaF, which had been planned originally (1. Progress Report, April 1978), was also dropped. The fluoride components and their

salts were carefully investigated by Schröder /2,3/, NaCl-$NaCO_3$-NaOH was deleted because of the difficult handling of NaOH--see section 5.2.

The test arrangement (Figs. 6 and 7) consists mainly of a high vacuum-pump stand with the necessary pressure measuring equipment, the recipient connected to it, a quartz glass tube containing the sample, a high frequency generator for inductive heating of the probe, as well as a NiCr-Ni thermo element needed for temperature measurement and a 2-channel servo-tension recorder for recording of the temperature curve against time. The recipient can be flooded with argon after evacuation to prevent any possible oxidation reactions. The two following schematic sketches (Figs. 8 and 9) will serve as illustration.

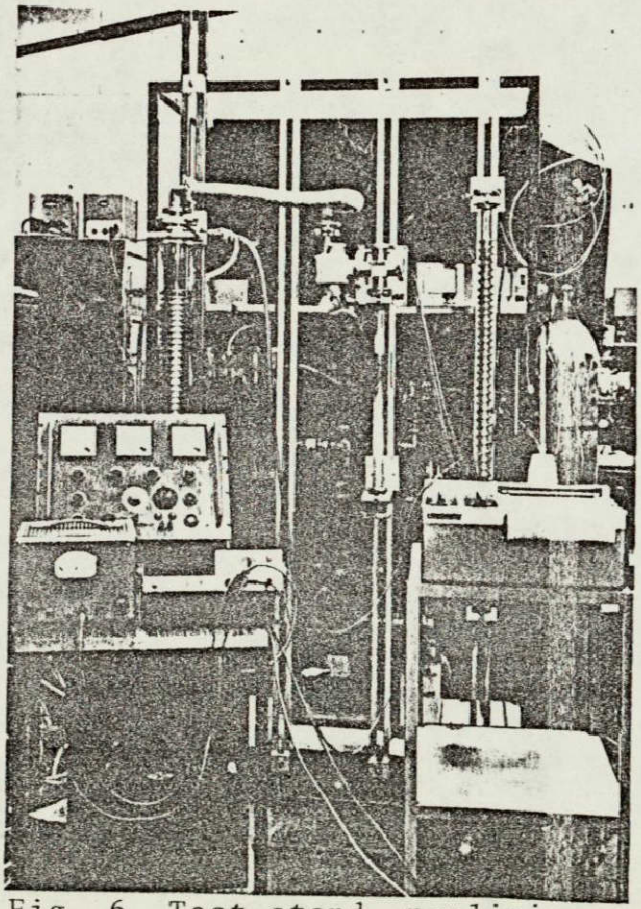

Fig. 6 Test stand, preliminary tests general view.

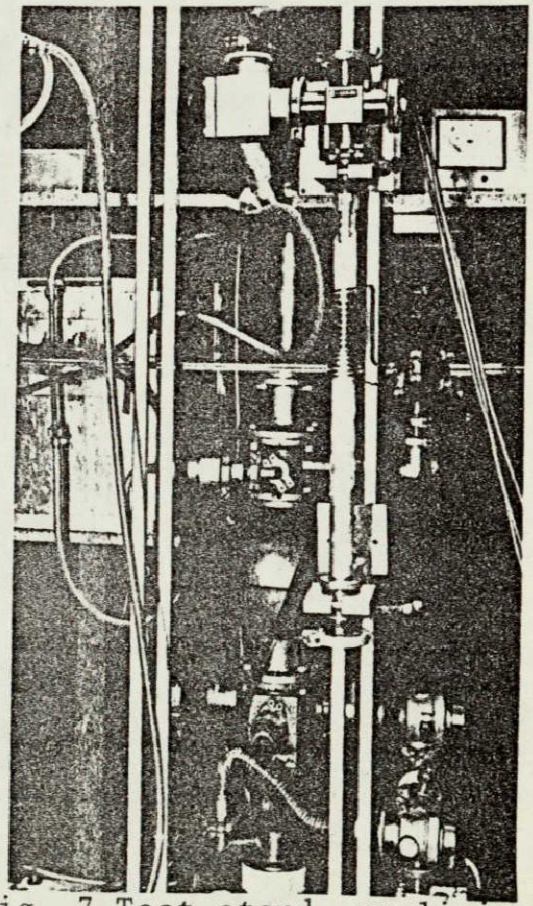

Fig. 7 Test stand, preliminary tests, recipient, induction coil, oil diffusion pump.

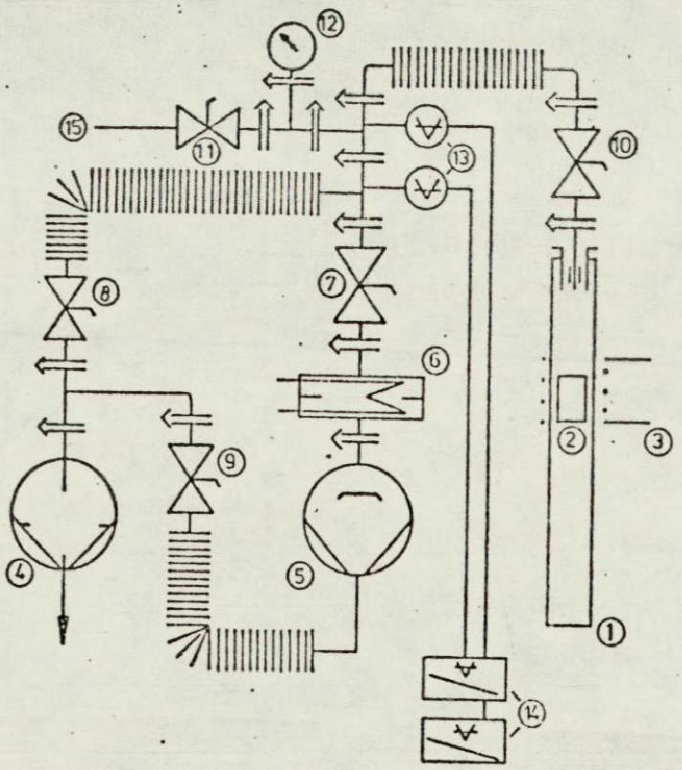

Key to numbers:

1	Recipient	6	Trap	14	Operating and insulating equipment for tubes
2	Sample holder	7	Valve		
3	HF-heating coil	8,9,10,11	Valves		
4	Fore pump	12	Manometer		
5	Oil diffusion pump	13	Vacuum test tubes	15	Argon connection

Fig. 8. Test stand--preliminary tests.

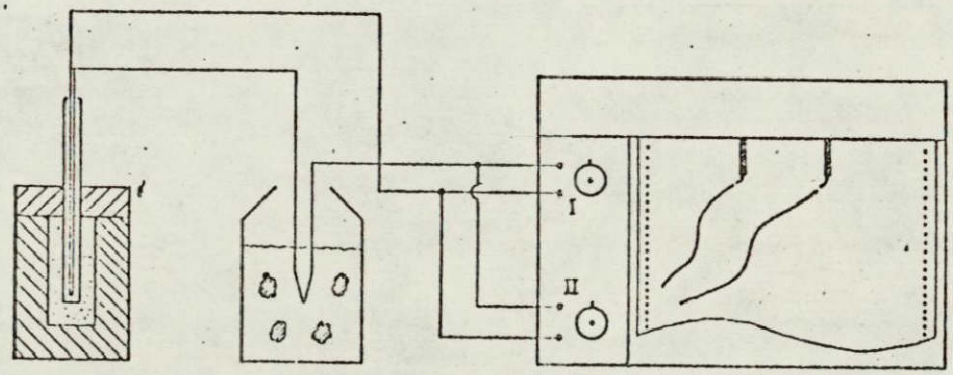

Sample with NiCr-Ni-thermo element	Ice water with NiCr-Ni-thermo element	2-channel tension recorder

Fig. 9. Temperature measurement equipment--preliminary tests.

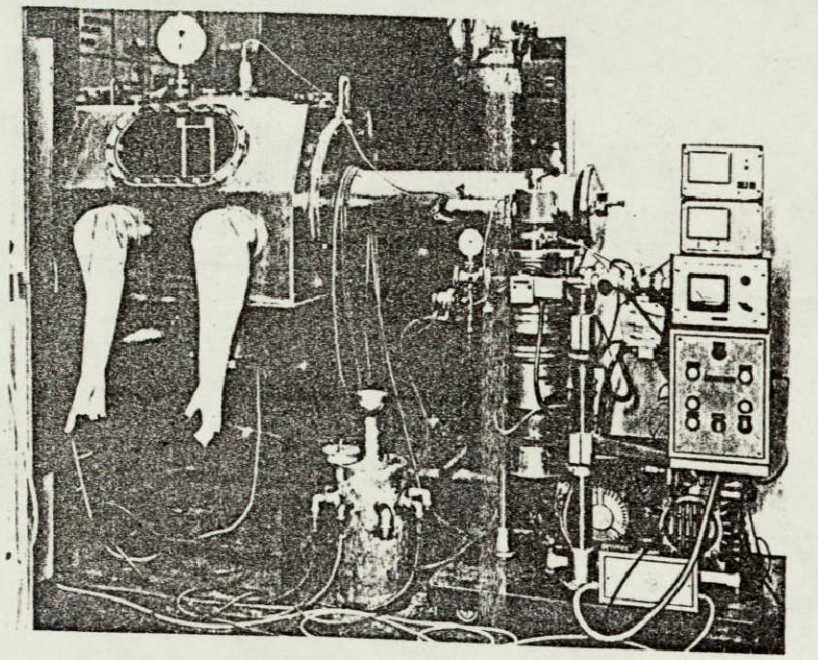

Fig. 10. Overall view: glove box for loading the sample container with vacuum pumps and control equipment.

After the sample container was loaded in a glove box flooded with Argon (Fig. 10) it was placed in the recipient which was evacuated to a pressure of about 10^{-4} torr. Subsequently, the evacuated space is flooded with argon up to a pressure of 800 torr. This slight excess pressure prevents the entrance of pollutants (particularly air) through possible leaks.

Heating is done inductively through a high frequency generator, with the output so regulated that a constant rate of heating results by the time the phase change occurs. During the cooling process power output is only slightly decreased to allow the sample to cool slowly. The thermal stress of the NiCr-Ni sleeve thermo-element (reference point ice water, i.e., 0°C) was switched in parallel to both channels of the voltage recorder so that one channel covers the less sensitive region without compensation while the other channel covering the

sensitive region is compensated up to a fixed temperature below the melting point of the sample. Therefore, sensitivity is the reason why the temperature curve of this channel shows more details, starting from the compensation temperature, than that of the other channel. Later on a printer with accurate division of the measurement region was used so that no compensation of the second channel was required.

Difficulties due to the experimental arrangement were caused, among other things, by poor regulation of the high frequency generator used for heating because of the small output powers required, i.e., the desired fine power adjustment, could not always be accomplished.

4.1.2 Results of the preliminary experiments

Figs. 11-23 show the heating and cooling curves plotted as recorded by pen, resp. printer. Two curves were recorded by the pen recorder, as described in 4.1.1, with the millivolt scale referring to the uncompensated channel. In addition, the power regulating the cooling is given in the cooling curves.

In the low temperature region only $NaNO_3$ of all pure compounds shows a predominant critical point. The melting temperature measured was 304°C, differing by 3°K from that given in /16/. No supercooling was measured. Due to rapid heating no critical point occurred in the heating curve. $ZnCl_2$ did not show the desired melting characteristics. It supercooled down to 255°C. Complete solidification occurred at 265°C and not for the values shown in the literature /14,15,16/. The cooling curve of NaOH shows no critical point, only a solidification interval of about 25 K. The liquidus temperature was 310°C, that of the solidus 285°C. For B_2O_3 no characteristic references for

a solidification point, resp. interval, were recognizable at all. B_2O_3 behaved like glass.

Of the mixtures investigated KCl-$ZnCl_2$ (51:49 mol-%) and KCl-$MgCl_2$-NaCl (20:50:30 mol-%) showed excellent solidification characteristics, though the latter has a small solidification interval of 4 K. The eutectic points were between 203°C and 336°C. $MgCl_2$-NaCl (38:62 mol-%) did show a pronounced critical point at 435°C but solidification already started above the eutectic temperature at 468°C. The mixture did not correspond to the eutectic composition so a melting interval of 33°K appeared. NaOH-KOH (64, 4:35, 6 mol-%) solidified between 232-216°C. No evidence of a eutectic point was seen during cooling. Heating and cooling curves for the mixtures often did not coincide, due to the fast inducting heating process.

Only pure salts were investigated for the high temperature region. $MgCl_2$ solidified at 712°C. That represents relatively good agreement with values from the literature. Pronounced supercooling was not measured. A melting interval seems to appear during heating. But the shape of this heating curve may also be due to the too fast heating, a function of the inductive heating process. NaCl solidified is an interval between 800-780°C. It solidified without supercooling. Melting occurred during a melting interval between 800-810°C. KF melted at 852°C. But solidification occurred in a solidification interval starting with a small critical point at 852°C and ending at 819°C. $NaCO_3$ melted at 848°C, but solidified similar to KF, in a solidification interval between 848 and 830°C. $NaSO_4$ had a melting and solidification interval. The width of the melting interval was 22°K, that of the solidification interval 20°K. The melting process started at 878°C and was over by 900°C.

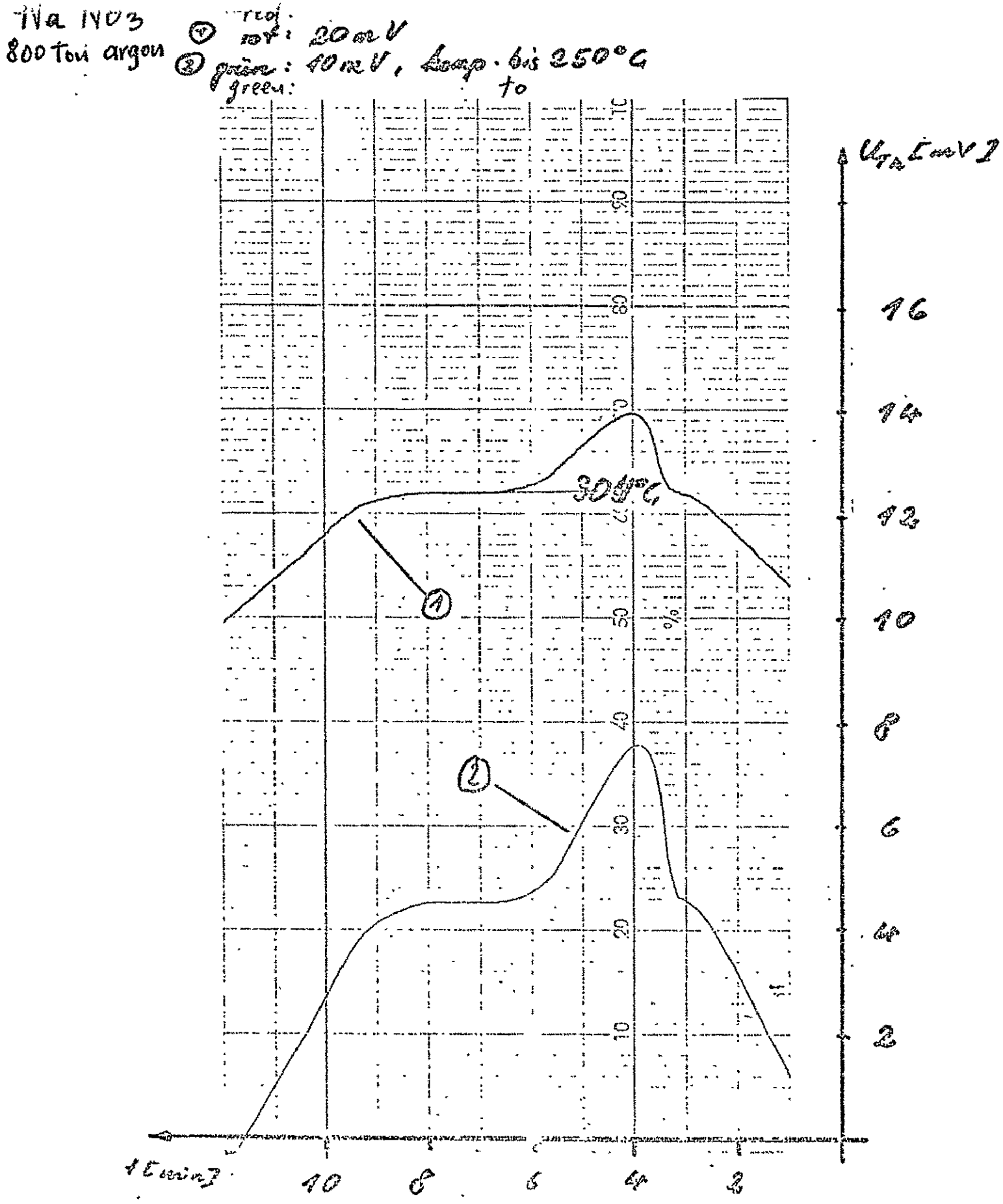

Fig. 11. Heating and cooling curve for $NaNO_3$.

 Bild 11: Aufheiz- und Abkühlkurve $NaNO_3$

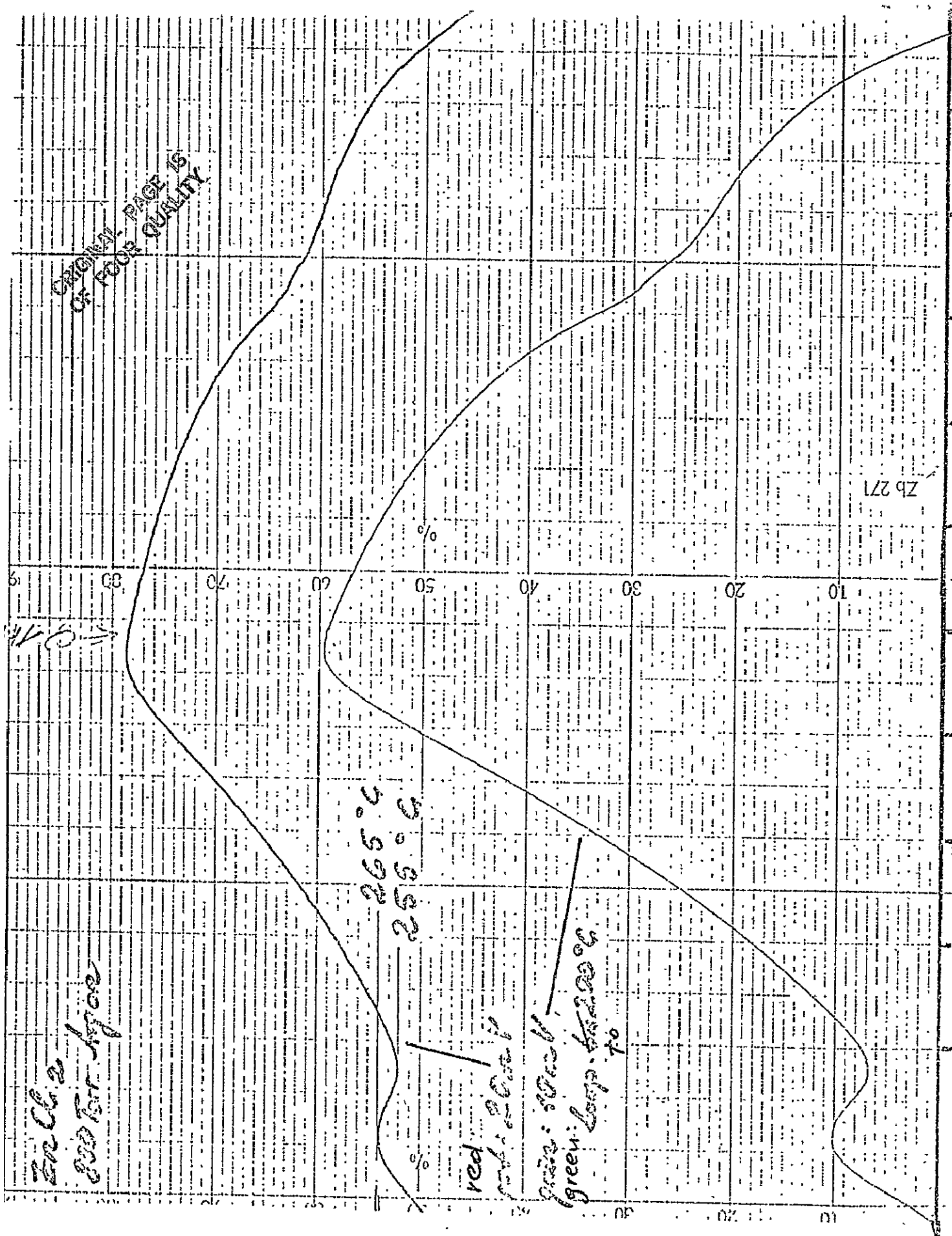

Fig. 12. Heating and cooling curve for $ZnCl_2$.

Bild 12: Aufheiz- und Abkühlkurve $ZnCl_2$

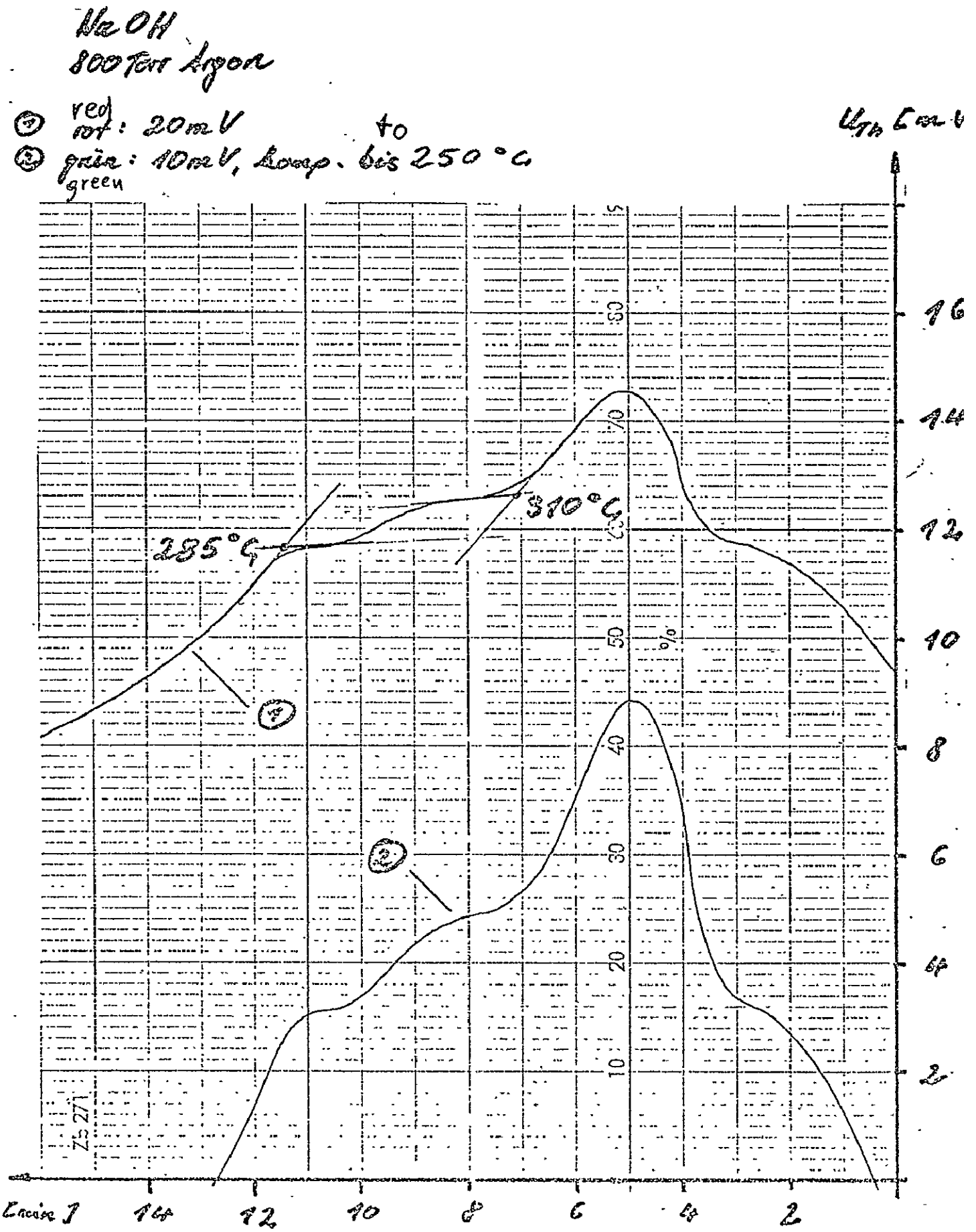

Fig. 13. Heating and cooling curve for NaOH.

Bild 13: Aufheiz- und Abkühlkurve NaOH

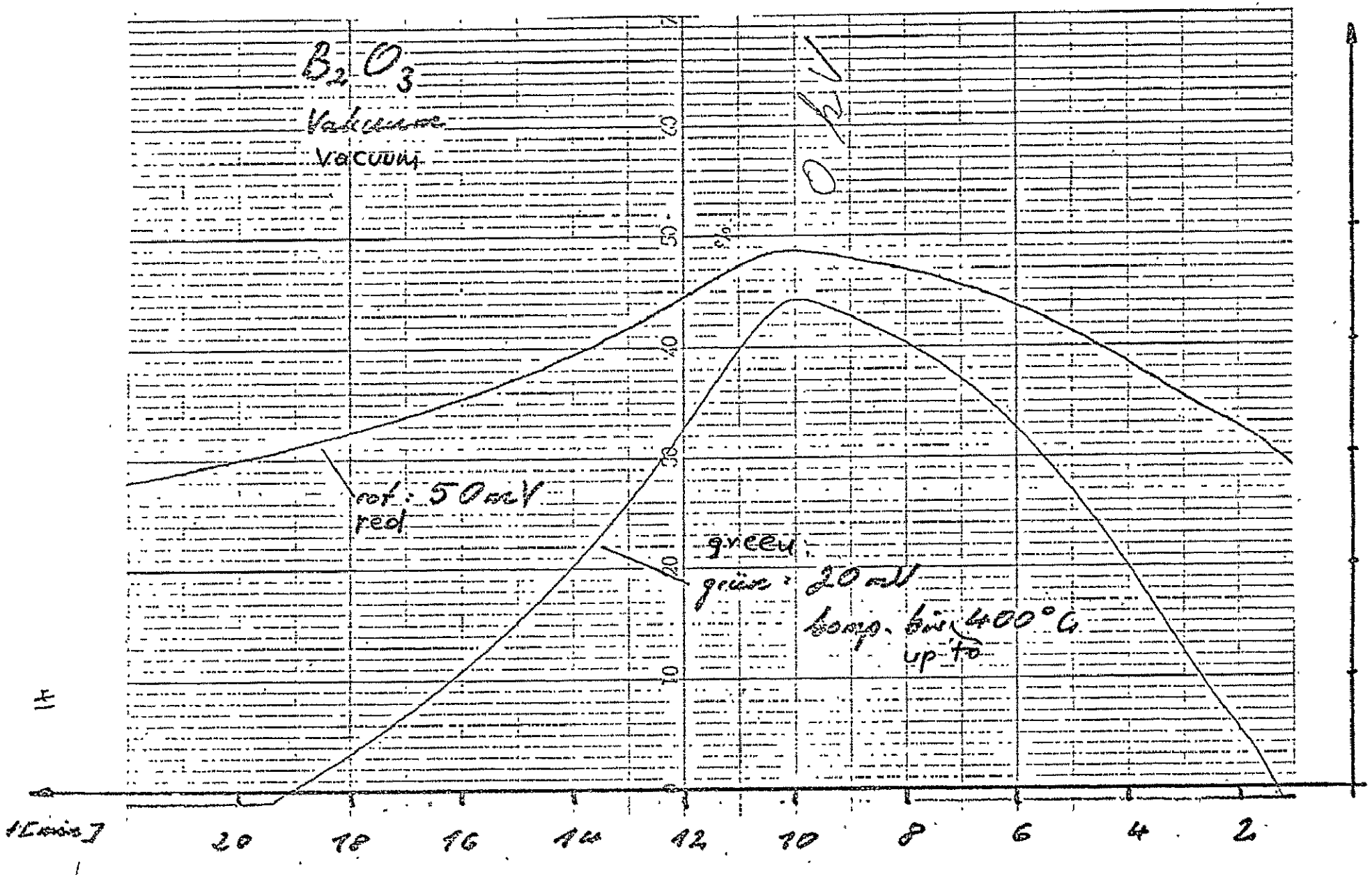

Fig. 14. Heating and cooling curve for B_2O_3.

Bild 14: Aufheiz- und Abkühlkurve B_2O_3

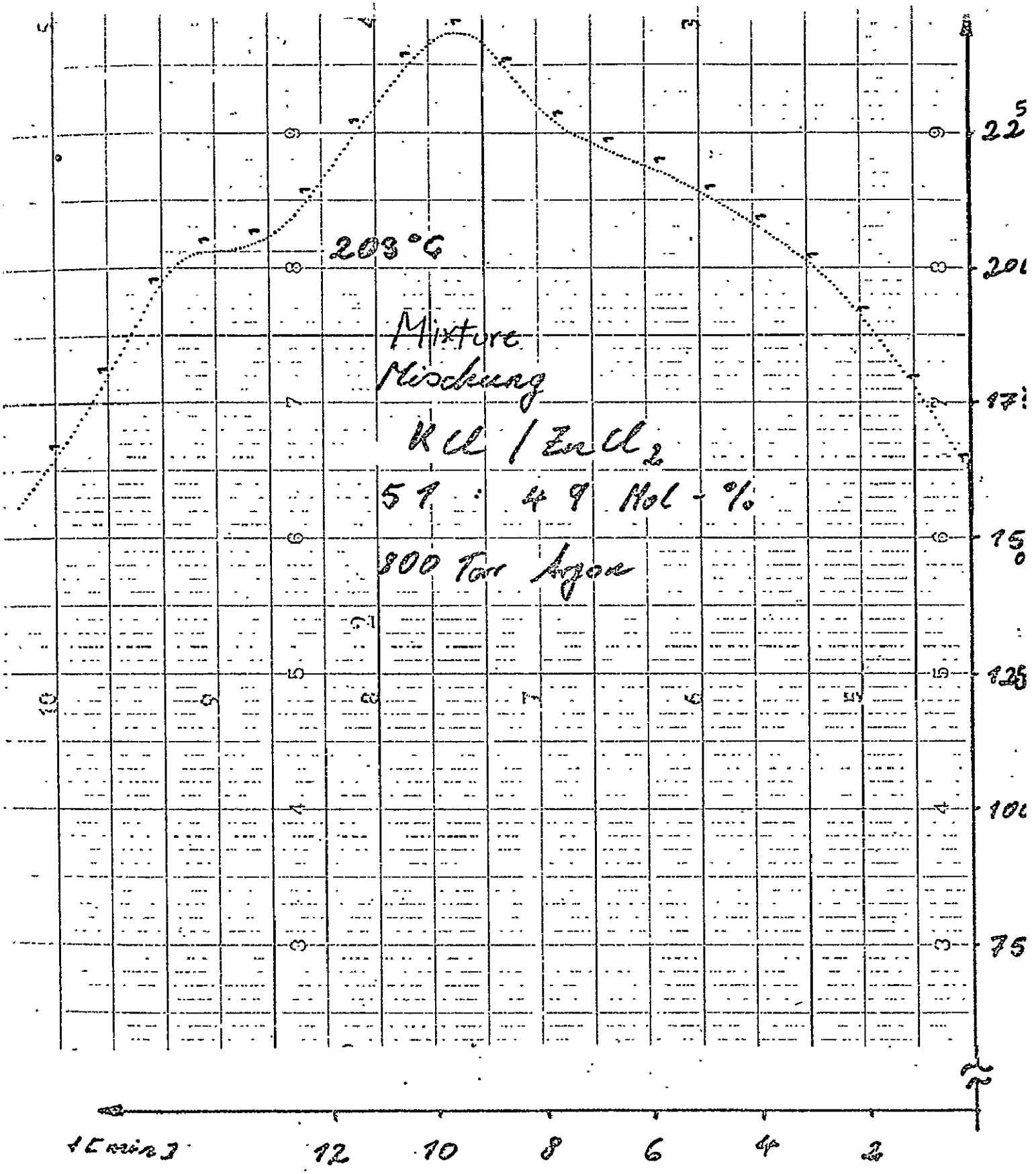

Fig. 15. Heating and cooling curve for $NaCl-ZnCl_2$.

Bild 15: Aufheiz- und Abkühlkurve $NaCl-ZnCl_2$

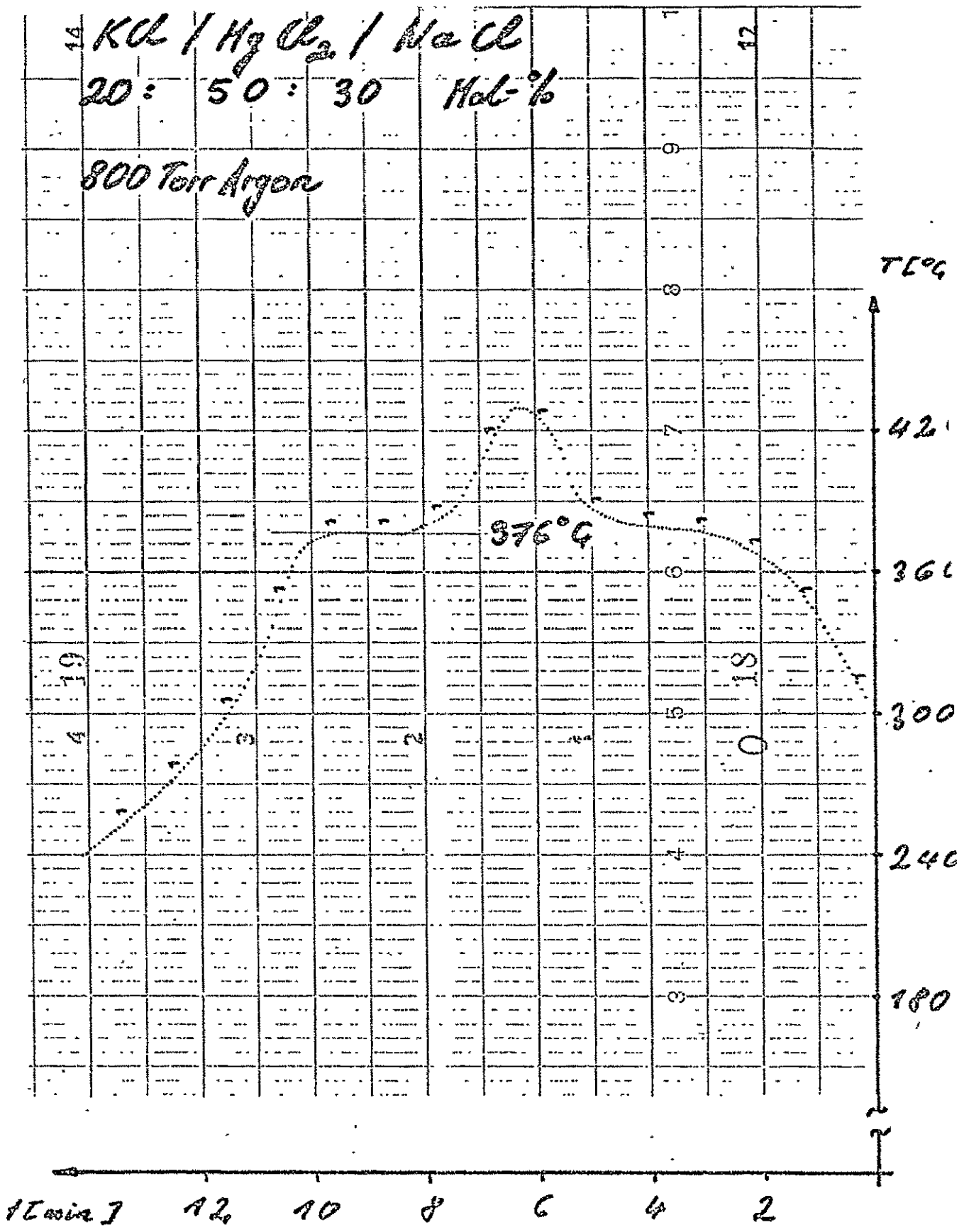

Fig. 16. Heating and cooling curve for KCl-$MgCl_2$-NaCl.

Bild 16: Aufheiz- und Abkühlkurve KCl-$MgCl_2$-NaCl

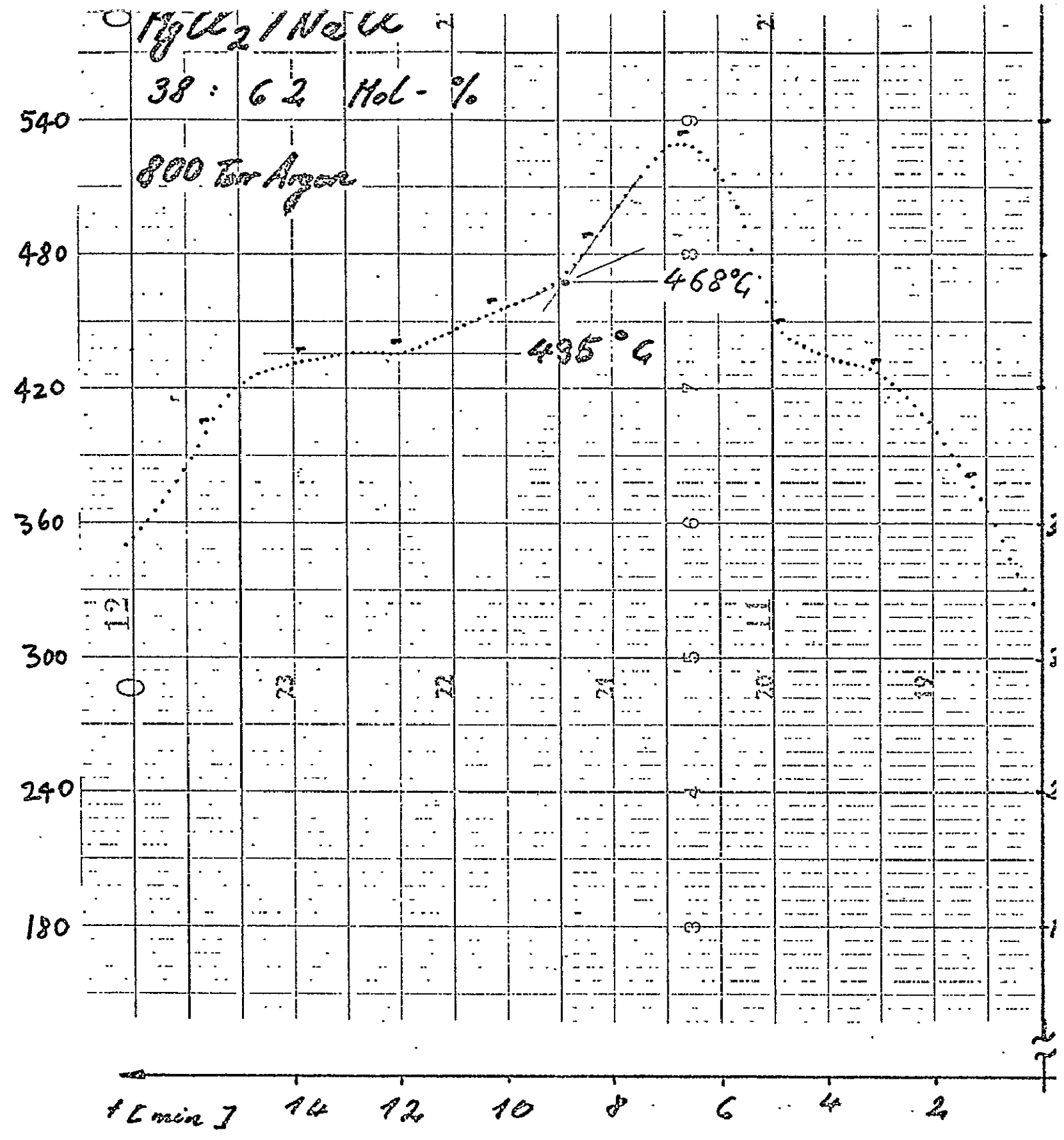

Fig. 17. Heating and cooling curve for $MgCl_2$-NaCl.

Bild 17: Aufheiz- und Abkühlkurve $MgCl_2$-NaCl

Fig. 18. Heating and cooling curve for NaOH-KOH.

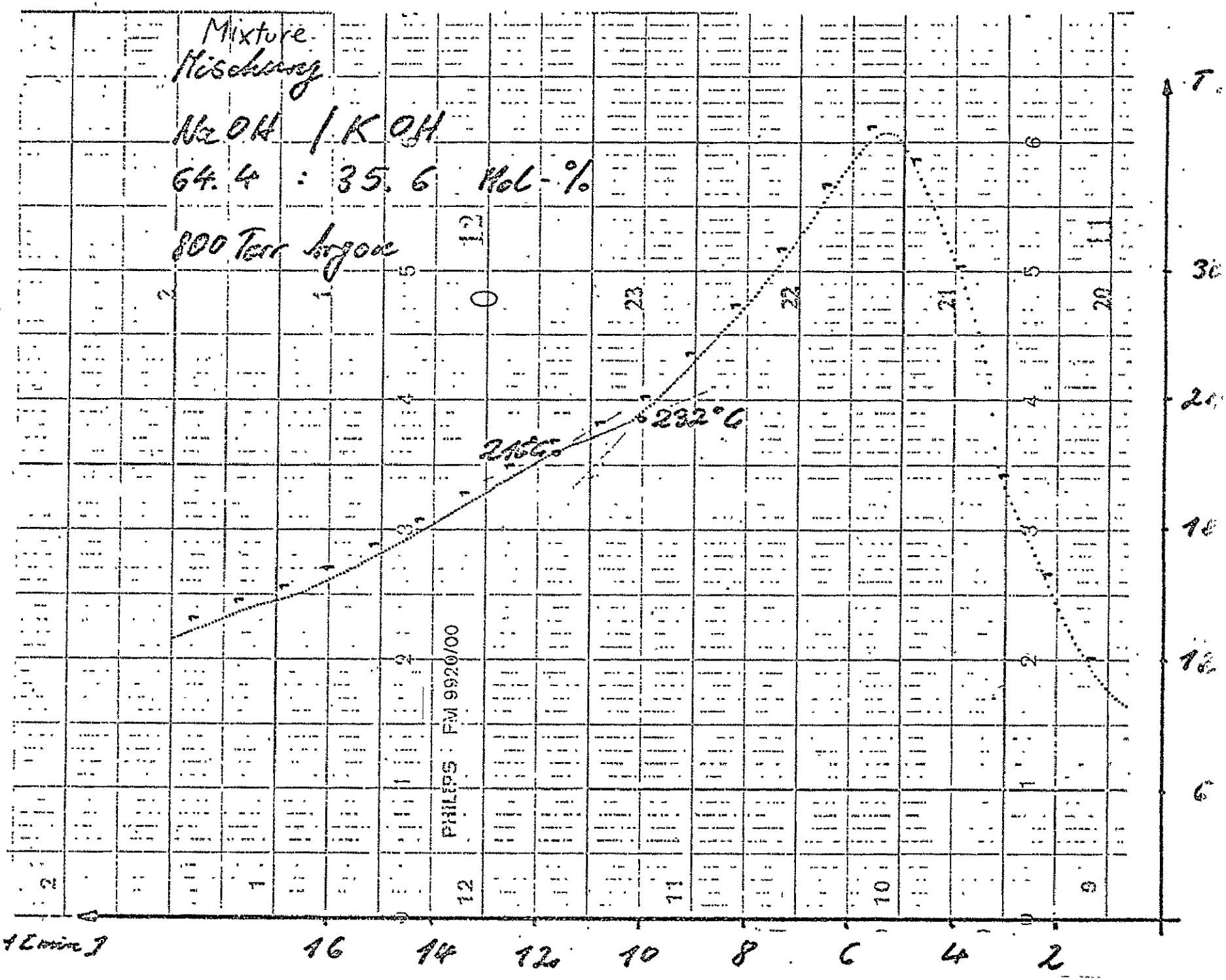

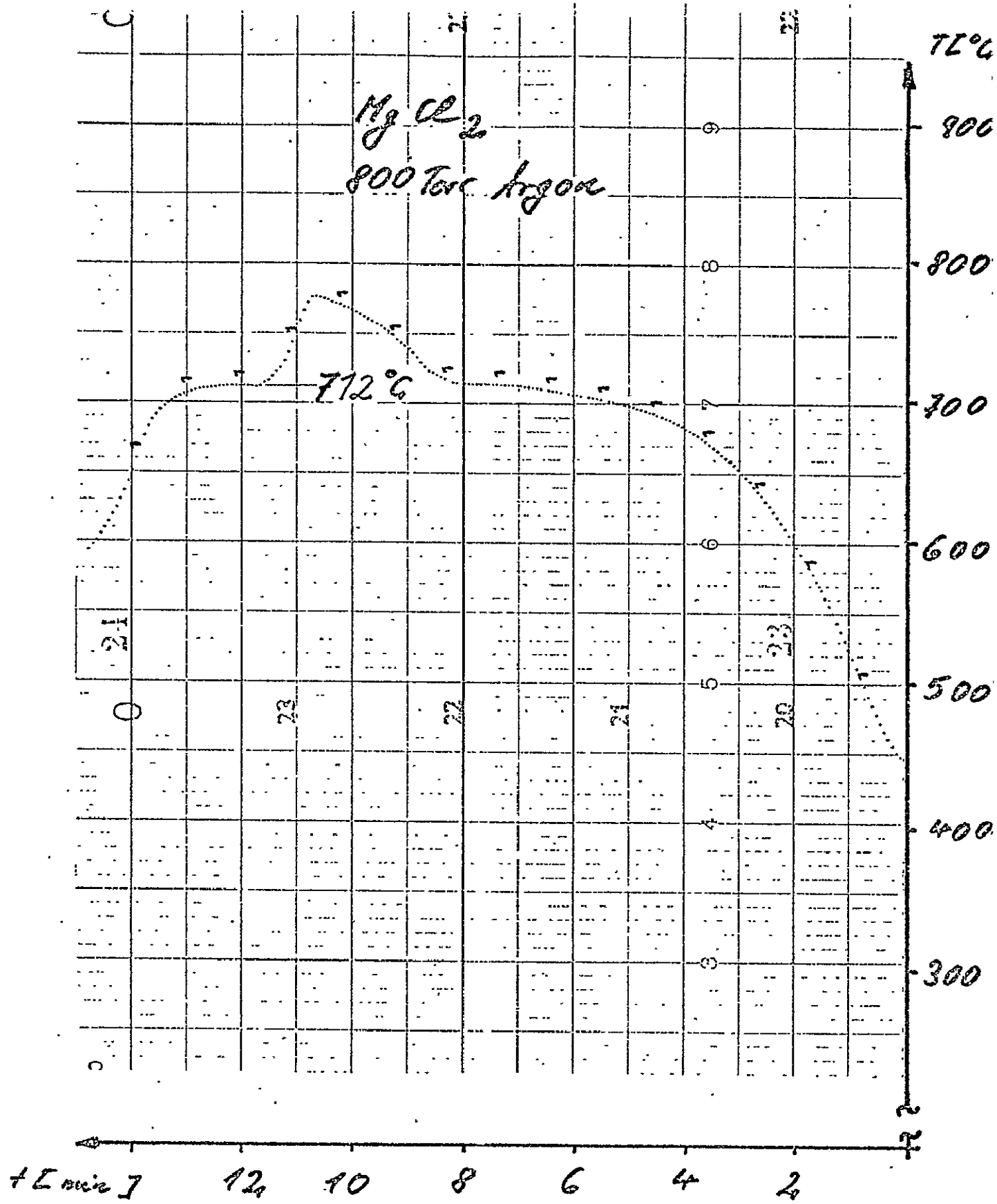

Fig. 19. Heating and cooling curve for $MgCl_2$.

Abb. 19: Aufheiz- und Abkühlkurve $MgCl_2$

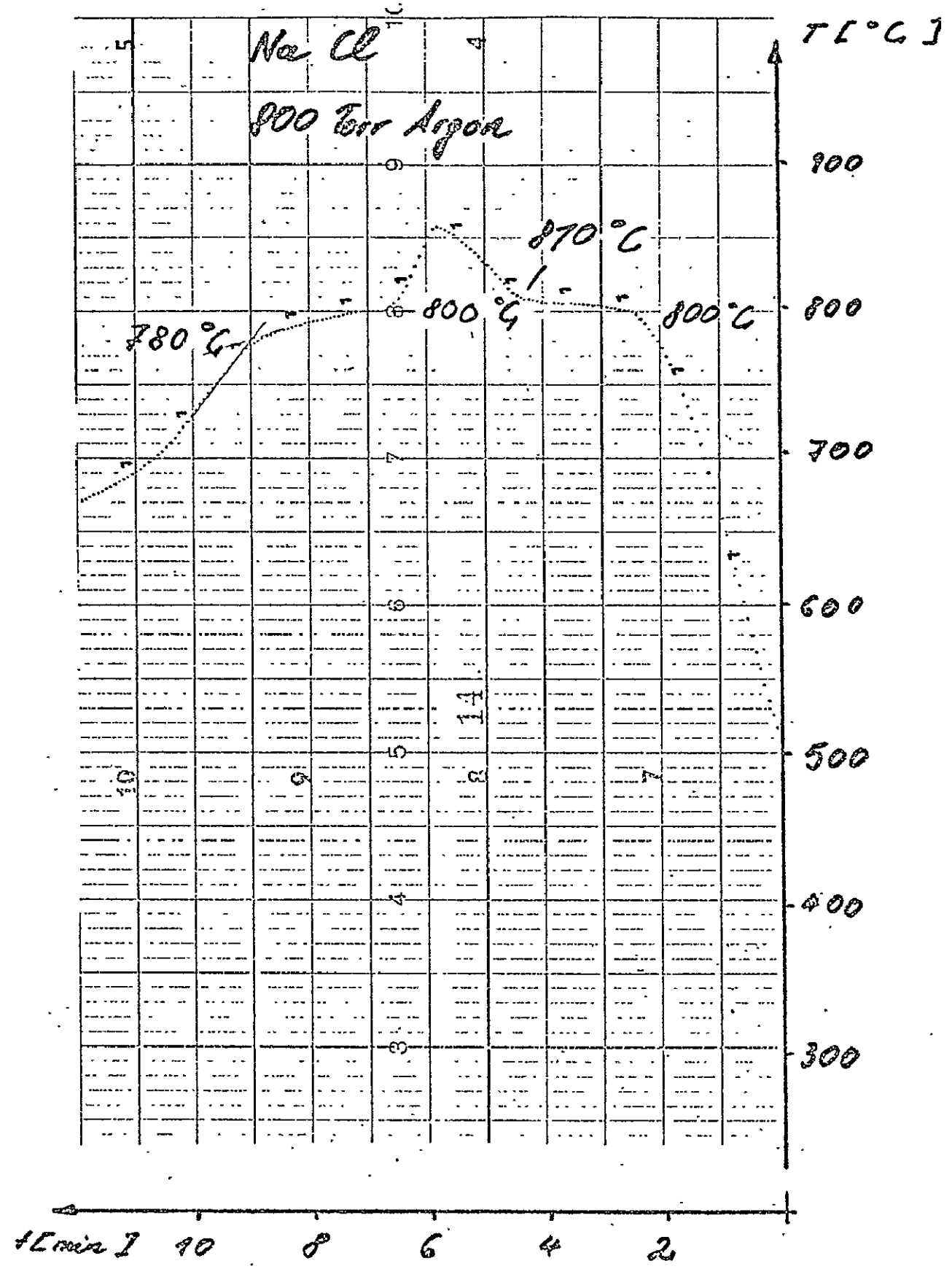

Fig. 20. Heating and cooling curve for NaCl.

Bild 20: Aufheiz- und Abkühlkurve NaCl

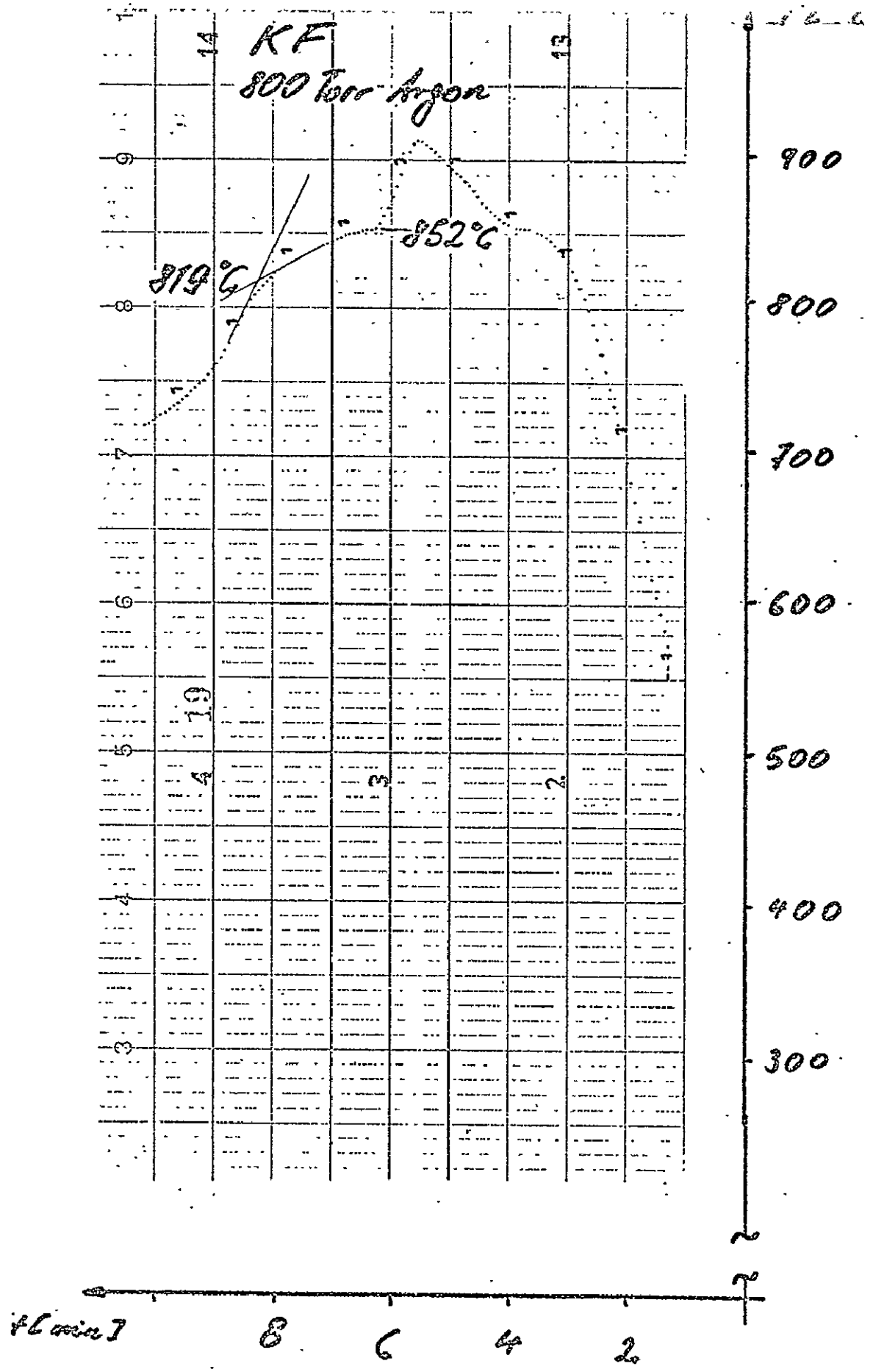

Fig. 21. Heating and cooling curve for KF.

Bild 21: Aufheiz- und Abkühlkurve KF

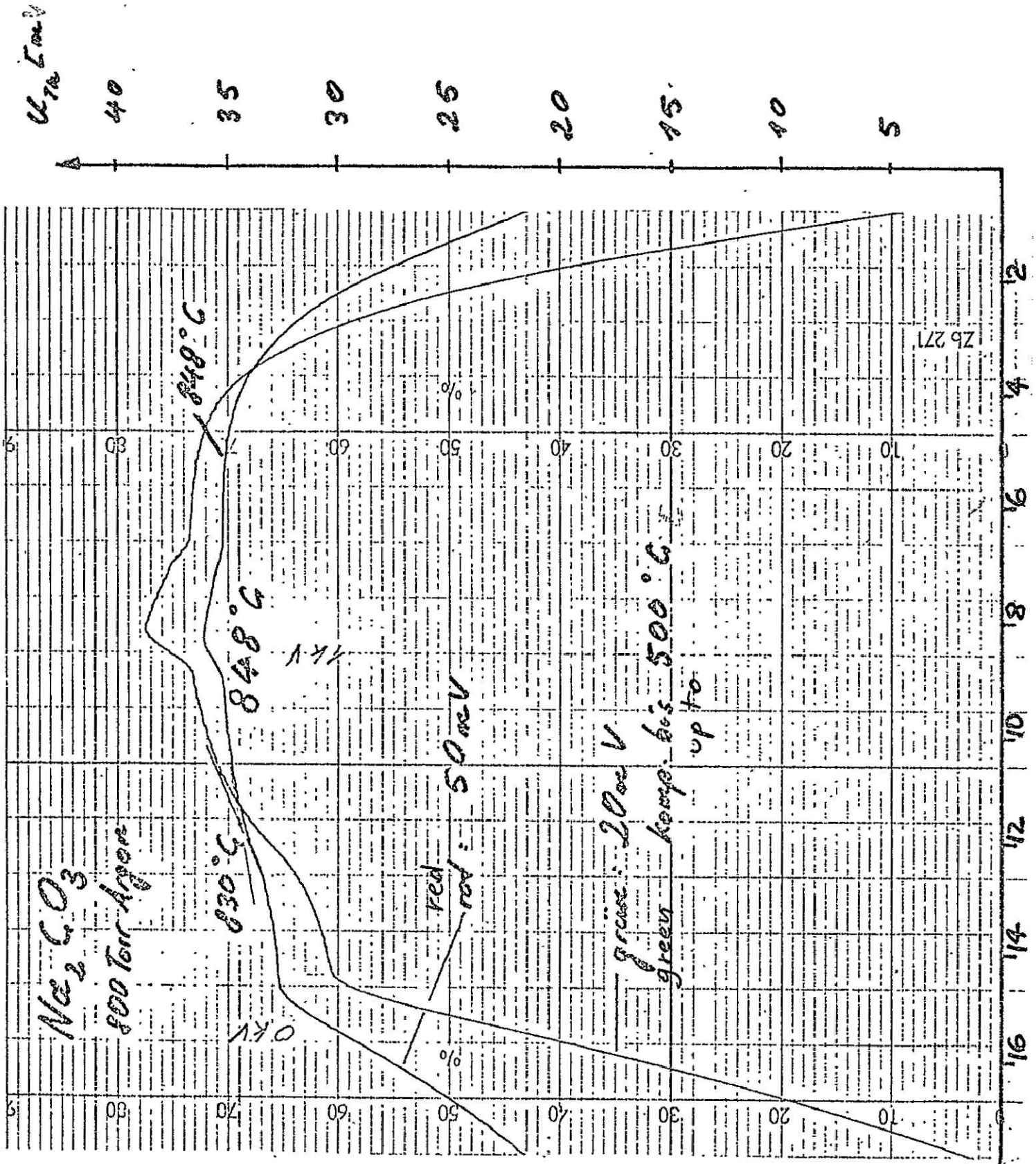

Fig. 22. Heating and cooling curve for Na_2CO_3.

Bild 22: Aufheiz- und Abkühlkurve Na_2CO_3

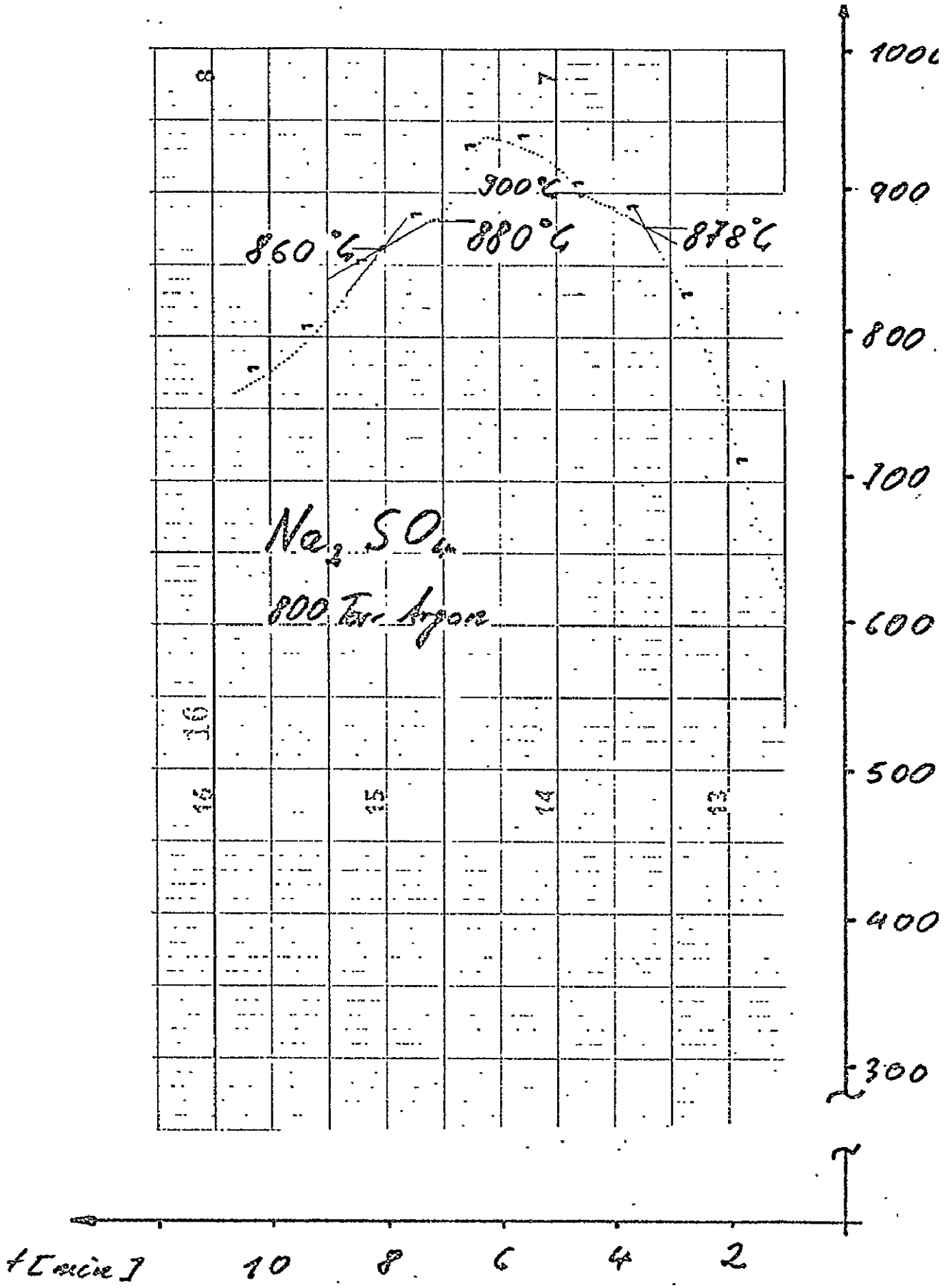

Fig. 23. Heating and cooling curve for Na_2SO_4.

Bild 23: Aufheiz- und Abkühlkurve Na_2SO_4

A few compounds were quite difficult to handle. NaOH, for instance, is very hygroscopic and its vapors are highly corrosive. That makes the loading process very difficult. $ZnCl_2$ is also very hygroscopic but is much easier to weigh and to load. The solidification interval was between 880-860°C.

4.1.3 Discussion of preliminary results and final selection of the storage materials

Test results have shown that there are often digressions from the data given in the literature. Melting and solidification periods occurred quite frequently even for pure compounds. These two phenomena may have their origins in impurities, even though the substances are delivered chemically clean from the manufacturer. Divergences in the mixtures are based on incorrect data of concentrations.

Supercooling was measured only for $ZnCl_2$. For all other materials nucleus formation set in at the melting point, resp. the liquidus point. That means that ideal conditions existed for heterogeneous nucleus formation. The wetting of the crucible wall by the compounds and their mixtures must have been good since no seeding crystals were added.

Decomposition could not be found either for sodium carbonate (Na_2CO_3) or for sodium nitrate ($NaNO_3$). It could not be clarified whether decomposition, resp. dissociation, led to the step-by-step solidification measured of sodium hydroxide (NaOH). Extensive investigations would have been required, of the kind that will be carried on during the cycle tests. No signs of dissociation were seen in other mixtures and compounds. The solidification behavior of B_2O_3 can be explained by its tendency to form glass-like, noncrystalline structures from the melt.

Based on the results obtained, $NaNO_3$, $KCl-ZnCl_2$ and $MgCl_2$-NaCl were chosen for service life and cycling tests. They cover the entire temperature range with their melting points. $KCl-ZnCl_2$ does not have a high melting heat but there are few other suitable salts or salt mixtures in the 200-210°C temperature range.

The mixture $MgCl_2$-NaCl (50/50 by weight-%) has a relatively broad melting period, but an attempt was made to reach the eutectic composition more accurately. Should that not be possible a mixture of three materials, $KCl_2-MgCl_2-NaCl_2$, must be used. Good melting and solidification characteristics and very high heat of fusion distinguish NaNO .

Three compounds, $MgCl_2$, NaCl and KFm, were further investigated for the high temperature region. $MgCl_2$ and NaCl have good melting and solidification characteristics and a high heat of fusion. A small solidification period was measured for KF. Since its melting point at 852°C represents a very interesting application temperature further tests must prove whether this is also true for slow cooling. Compared to Na_2CO_3 and Na_2SO_4, also interesting because of their high melting points, KF has a higher heat of fusion. In addition it is not desirable to run the risk of thermal decomposition, which was observed in carbonates, through the use of Na_2CO_3.

4.2 Service life tests

Tests of service life examine the compatibility of melted storage materials and construction materials.

The combinations marked x in Tables 10 and 11 were investigated in both temperature regions.

Table 10

Combination of Storage Material/Construction Material
Medium Temperature Range (200°C-450°C)

Construction Materials / Storage Materials	St 35 St 37	13CrMo44	CuNi30Fe	Ni67Cu
$KCl-ZnCl_2$	x	x		x
$NaNO_3$	x	x	x	
$MgCl_2-NaCl$		x	x	x

Table 11

Combination of Storage Material/Construction Material
High Temperature Region (600°C-950°C)

Construction Materials / Storage Materials	1.4828	1.4876	2.4630	2.4816
$MgCl_2$	x	x	x	
NaCl		x	x	x
KF		x	x	x

The salts were filled into cylindrical containers of the chosen construction materials. A sample of the same material in sheet form is always added. The containers (Fig. 24) are welded shut by electron beam welding. Heating takes place in electrically heated chambers. Temperature regulation is thermoelectric,

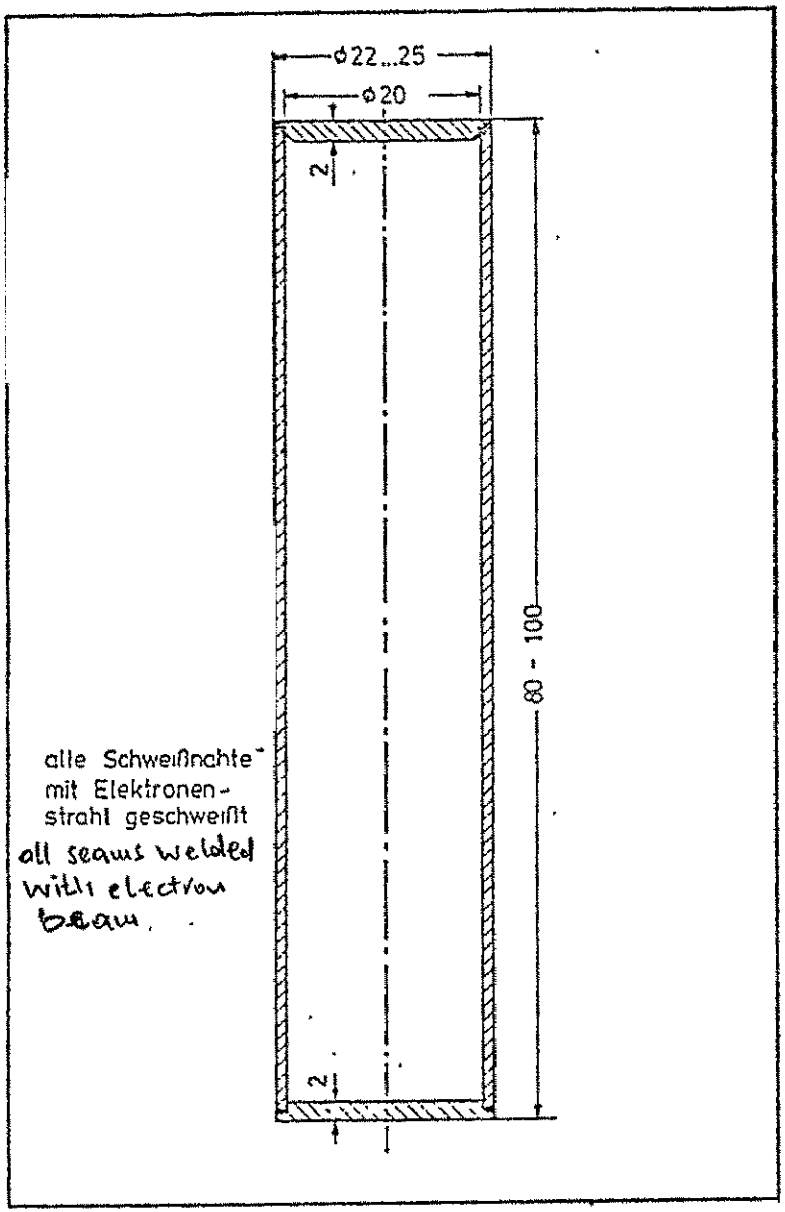

(a) Service life tests
(a) Lebensdauerversuche

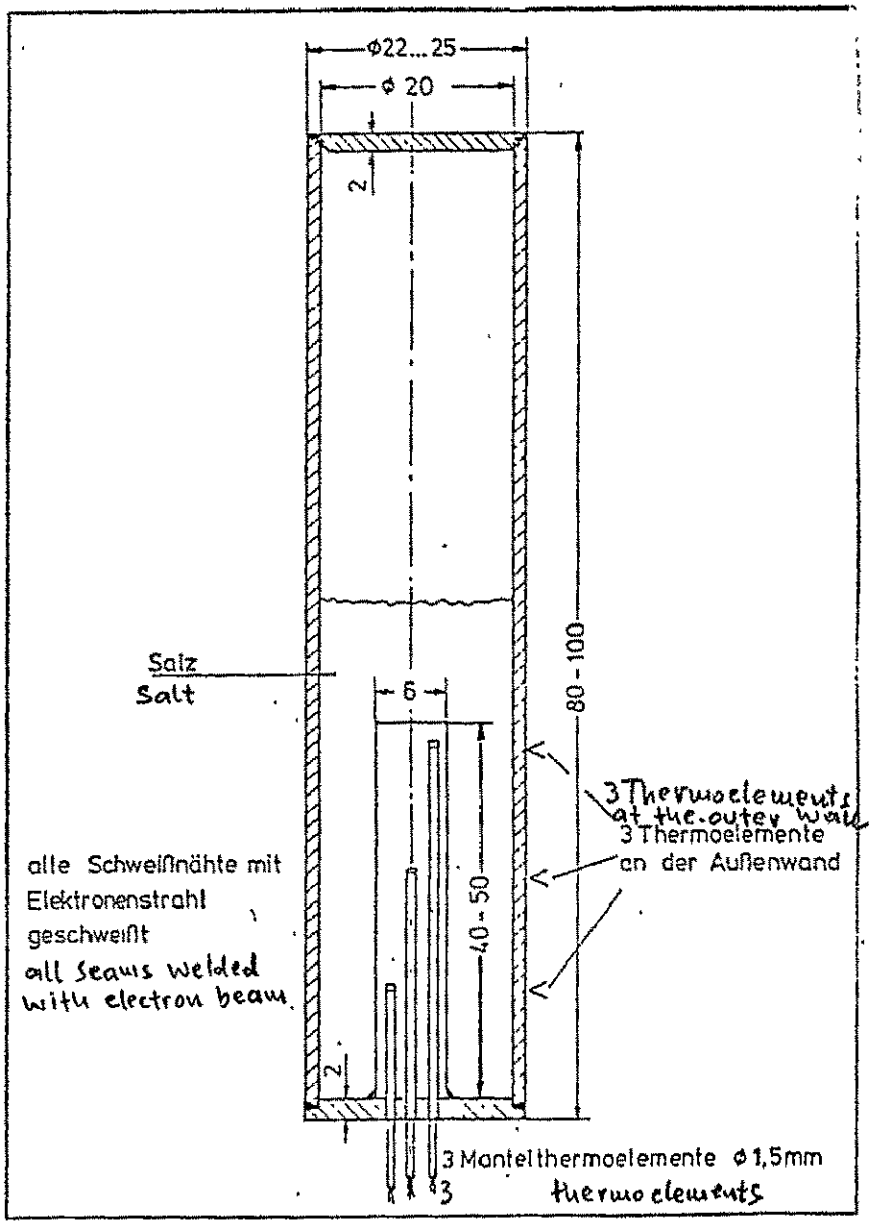

(b) Cycle tests
(b) Zyklustests

Fig. 24. Test container.

Bild 24: Versuchsbehälter

fully electronic via PID-controls and steady output via thyristors.

In each case the test temperature is 50°K above the melting temperature. Five different test periods (500, 1000, 2000, 4000, and 8000 hours) per combination are planned. Three containers and three sheet samples will be tested for each storage material, for each construction material and for each time period.

The sheet samples serve for measurement of weight differences. Through them loss of mass is to be determined. It will thus be possible to calculate the rate of loss of mass and the rate of removal. The type of corrosion will be determined through examinations of the inner wall of the container and of the sheet sample surfaces by means of light microscopes and electron scan microscopes. The composition of resultant corrosion products is determined through chemical analyses. The influence of ongoing corrosion on the melting behavior, will be investigated through recording of heating and cooling curves.

4.3 Cycling tests

4.3.1 Test arrangement and test performance

The cycling tests serve for examination of thermal stability. Repeated melting and solidification cycles (100 runs) serve to establish whether behavior of the storage materials changes during melting is affected.

After evaluation of the first service life tests, the most corrosion resistant material is used for each salt to construct containers for the cycling tests. The containers are equipped with six thermo-elements, as shown in Fig. 24. Such an arrangement permits measurement of the temperature distribution

in the salt, as well as evaluation of its thermal conductivity. By means of these thermo-elements heating and cooling curves can be recorded during each melting and solidification cycle. That permits immediate detection of changes in the melting behavior.

The melting and solidification cycle is to run during the temperature interval $T_S \pm 50°K$. The salts are heated in electrical heating chambers for that purpose. The walls of the kiln are so designed that alternate annealings are possible with linear cooling from a maximum 100°C/h to lowest temperatures of 200°C (three kilns) and 650°C (three kilns). The nominal temperatures of the kilns are 500°C and 950°C. Two electronic program transmitters are built in for cycle control, one for medium temperature range and one for the high temperature range. The control equipment permits operation of each kiln in the nominal region with a different temperature; alternate values (cycle length) and dwell time at the upper and lower terminal temperatures are the same. The basic equipment of the kilns is the same as for the service life tests. There is a kiln with three containers for each salt.

Acquisition of test data (Fig. 25) is carried out directly through a laboratory computer PDP 11/40. Temperature measurement is made with NiCr-Ni thermo-elements and with a digital pyrometer model 267 by the Newport Company (ADC). This instrument has a built-in temperature compensator as well as an A/D converter. Mercury multiplexers, which permit measurements in the millivolt region, are connected in series with the test instruments. This permits acquisition of test data from all 108 thermo-elements with a relatively small number of test instruments (six). From the test instrument the data are passed on to an intermediate storage where the conversion from BCD to ASCII also takes place. From here the data pass through a parallel/series converter to the computer. A time control device

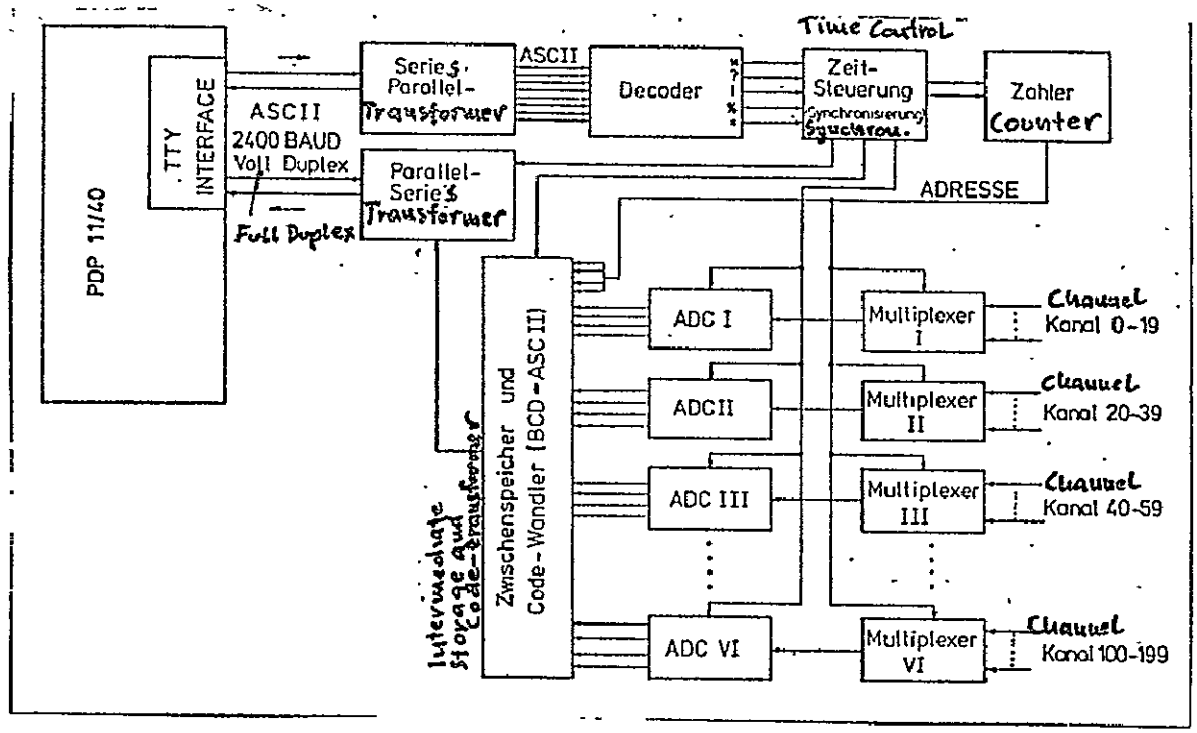

Fig. 25. Block diagram of data acquisition arrangement.

synchronizes the data acquisition between multiplexer, ADC and intermediate storage. The counter records the test channels used. The proposed arrangement permits simultaneous measurements from six thermo-elements. This allows simultaneous interrogation of all thermo-elements of a container at the same time, a matter of importance for capacity evaluations and determination of temperature distribution in the storage medium.

4.3.2 Data acquisition and evaluation

For service life tests at constant temperature only control of the temperature stability is required. Monitoring of that stability can be carried out simultaneously with the periodically required visual monitoring of individual samples. Sample temperatures are measured with a thermo-element. Temperature indication can be made through an analog instrument or a digital indicator.

Acquisition and evaluation of temperatures for the cyclical service life tests is far more complicated. A great many temperatures must be recorded for determination of heating and cooling curves of individual samples, which are further processed by means of a computer program on EDP equipment.

The program serves on the one hand for determination of the shape of heating and cooling curves and on the other for determination of the melting temperature, resp. solidification temperature, of the storage material from the shape of the curves. Variations of individual curves give information about changes occurring in the melting or solidification behavior. A significant part of the program serves for determination of the storage material melting temperature. Progress of the melting front from the outside to the inside of the sample container leads to a heating curve profile which does not agree with the ideal curve profile. The melting temperature designated as T_S in Fig. 26 must be determined by computation.

The program of evaluation consists of two different parts: one is organizational and the other is numerical.

In the organizational part each measurement is supplied with a number. The samples are given consecutive numbers from 1 to 18. Numbers are assigned to the samples in such an order that samples 1 to 3 belong to kiln 1, samples 4 to 6 to kiln 2, etc. In addition there is the possibility of indicating which salt is contained in the individual samples. During operation for a long period the possibility exists that poor contact of a thermo-element with the container wall would result in the indication of wrong temperatures or in no indications at all. For that reason a field with eighteen rows and six columns is provided in the program. Each of the 108 field elements represents a thermo-element (18 rows = 18 samples, 6 columns = 6 thermo-elements).

By placing a 0 in an element the computer is told not to interrogate that thermo-element. A number 1 means interrogation. In the organizational part the start and finish of a test series are put in and the time intervals between individual tests.

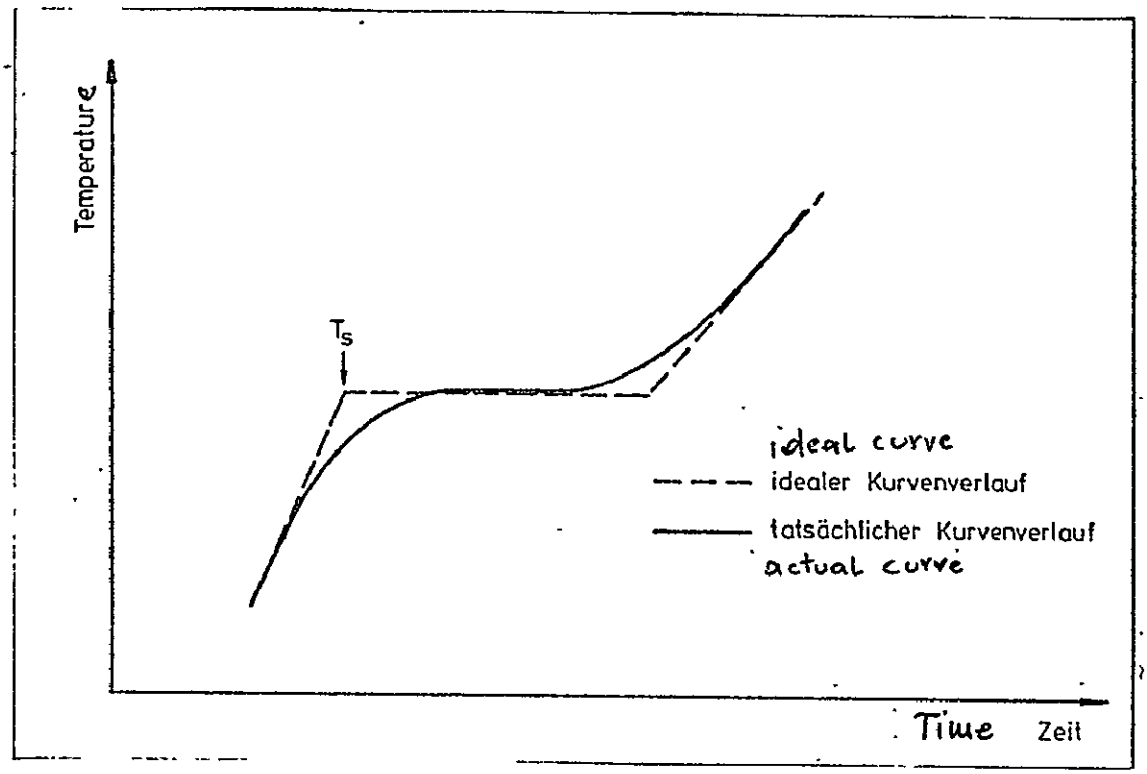

Fig. 26. Definition of the melting temperature.

In the numerical part of the program the melting temperature is determined. It was shown that each heating and cooling curve has only one turning point. A third order polynomial is formed by the test data recorded. A polynomial of the third order also shows only one turning point and reproduces the characteristics of the heating and cooling curves very well. The polynomial is generated according to the method of least squares. The tangent to the turning point is determined for the polynomial generated. As shown in Fig. 26, the temperature at the intersection of two tangents is given as the melting temperature. One

tangent is the turning tangent the other one is placed against the heating curve so that its point of contact with the curve comes before the point of maximum curvature. This method is applied in daily practice. For determination of the melting temperature through computation a method was developed in which the condition is met that the second tangent must touch the heating curve before the largest curvature. The definitive tangent is determined by iteration (see Fig. 27). The first tangent is placed against the curve at the point with abscissa

$$t_1 = \frac{t_A + t_B}{2} .$$

The initial point of measurement, shown by t_A and t_B, is so chosen that the corresponding temperature is 5°K below the temperature in the turning point. This guarantees that the definitive tangent will touch the curve in the desired region. The intersection of the tangents with the turning tangent is designated as t_C. The second tangent is placed at the point with the abscissa

$$t_2 = \frac{t_A + t_C}{2} .$$

This method is repeated so long until the abscissa change of two tangent intersection points t_n and t_{n+1} has fallen below a required degree of accuracy. The temperature so determined is given as melting temperature.

It is planned to print out the measured temperatures and to store only the coefficients of the third order polynomial in the computer. That will take up much less storage capacity in the EDP-equipment.

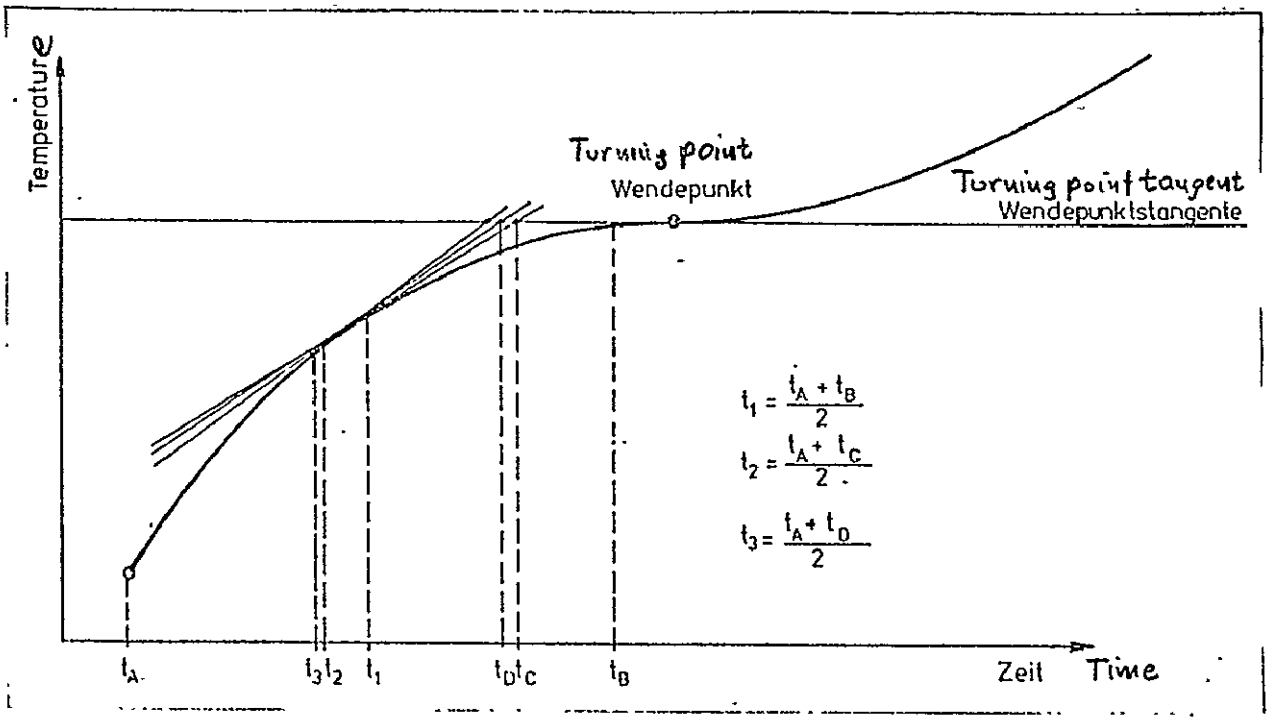

Fig. 27. Determination of melting temperature.

References

1. Laing, N.: Kristallisations-Wärmespeicher und deren Anwendung (Crystallization heat accumulators and their application), VDI-Bericht Nr. 223, 1974, S. 49

2. Schröder, J.: Energiespeicherung in Form von Wärme (Energy storage in form of heat), VDI-Bericht Nr. 223, 1974, S. 67

3. Schröder, J.: Thermische Energiespeicherung; Symposium III, Krafterzeugung mit Sonnenenergie und Langzeitspeicherung (Thermal energy storage; Symposium III, power generation with energy and long-term storage), Hotel International, Zürich, 1975

4. Lane, G. A., and D. N. Glew: Heat-of-Fusion Systems for Solar Energy Storage, Proceedings of the Workshop on Solar

Energy Storage Subsystems, Charlottensville, Virginia, USA, April 1975

5. Green, R. M., D. K. Ottesen, J. J. Bartel, P. P. Bramlette: High Temperature Thermal Energy Storage, Sharing the Sun, Solar Technology in the Seventies, Joint Conference, American Section ISES and SES of Canada, 1976, Winnipeg, Canada, Vol. 8

6. Tye, R. P., J. G. Bourne, A. O. Desjarlais: Thermal Energy Storage Material Thermophysical Properties Measurement and Heat Transfer Impact, NASA-Report No. NASA-CR-135098, 11. August 1976

7. Böhm, H.: Einführung in die Metallkunde (Introduction to metallurgy), BI-Hochschultaschenbuch 196/196 a, Mannheim 1968

8. Haasen, P.: Physikalische Metallkunde (Physical metallurgy), Springer Verlag, Heidelberg, 1974

9. Schatt, W.: Einführung in die Werkstoffwissenschaft (Introduction to materials science), VEB Deutscher Verlag für Grundstoffindustrie, Leipzig 1972

10. Uhlig, H.: Korrosion und Korrosionsschutz (Corrosion and corrosion protection), Akademie Verlag Berlin, 1970

11. Evans, U. R.: Einführung in die Korrosion der Metalle (Introduction to the corrosion of metals), Verlag Chemie Weinheim/Bergstr., 1965

12. Engell, H. J.: Verfahren zur Messung der Auflösungsgeschwindigkeit korrodierender Metalle in lufthaltigen

Lösungen (Method for measurement of the rate of decomposition of metals in solutions containing air), Archiv für Eisenhüttenwesen, Heft 9, September 1958, S. 553

13. Dechema-Werkstofftabellen (Tables of materials), Frankfurt

14. D'Ans: Chemiker Taschenbuch (Handbook for chemists), 3. Aufl., Bd. 1

15. Gmelin: Handbuch der anorganischen Chemie (Handbook of inorganic chemistry), Verlag Chemie, Weinheim, 1974

16. West, R. C.: Handbook of Chemistry and Physics, The Chemical Rubber Co., Cleveland, Ohio, 1968

17. Rabold, E.: Corrosion Guide, Elsevier Publishing Company, Amsterdam, 1968

18. VDM-Taschenbücher (pocket handbooks)
    (a) Cronifer-Crofer
    (b) Nicrofer
    (c) Nicorros

19. Richter, F.: Die wichtigsten physikalischen Eigenschaften von 52 Eisenwerkstoffen (The most important characteristics of 52 iron materials)

20. Wellinger-Gimmel: Werkstofftabellen der Metalle (Tables of materials for metals), A. Kröner Verlag, Stuttgart, 1963

21. Clark, V. P., C. D. Dean: Fused Salt Mixtures: Eutectic Compositions and Melting Points, Bibliography 1907-1968, Fused Salts Information Center, Sandia Laboratories, Report No. SC-R-68-1680, December 30, 1968